Land Cover Change Analysis in Tropical Forest Ecosystems Using GIS and Remote Sensing: The Kakum Conservation Area (KCA) of Ghana as a case study.

CANDIDATE NUMBER: 180766

WORD COUNT: 13,248 (excluding references)

Dissertation submitted in partial fulfillment for the award of the degree of Master of Science in Environmental Change and Management, University of Oxford.

SUBMISSION DATE: 2nd September, 2013.

ABSTRACT

The primary objective of this study was to evaluate and map the land cover dynamics that had taken place in the KCA over the past three decades as a result of the changes in land use and land tenure systems. To analyse these changes, change detection techniques based on remote sensing data (Landsat TM and ETM+) were used. The change detection algorithms that were adopted for this study include Principal Component Analysis, Univariate NDVI Image Differencing and image classification analysis. These methods were quite complementary in their results. The PCA helped in the determination of areas of possible changes, the Image differencing algorithm was able to highlight the land cover change trajectories and the Post-classification approach was able to highlight the trends in land cover changes in each land cover type in the area.

Through the knowledge gained during fieldwork and by overlaying the land use map of the area onto the results of these change detection algorithms, the study was able to link the observed land cover dynamics to the changes in land use systems in the area. Notable among the shift in land use practices which contributed to the observed land cover changes, mainly the introduction of cultivation agriculture in the area by immigrating cocoa farming communities-leading to the clearance of forests to give way to farms, mainly in close proximity to the Kakum-Attandanso forests.

DECLARATION

Except where indicated, I declare that this is my own unaided work and is less than 15,000 words in length. I confirm that any assistance is explicitly acknowledged and any material drawn from secondary sources is explicitly referenced.

Signed………………………..   Date…………………

ACKNOWLEDGEMENTS.

I am particularly grateful to Professor Yadvinder Malhi, my supervisor for his help in spite of his heavy schedules. Many thanks also to Dr. Tom Thornton my course director for his support, suggestions and useful comments. They have given meaning to this research. Also worth mentioning is Dr. Booker Ouma Ogutu of the University of Leicester for his valuable support in the practical GIS/Remote sensing work.

My gratitude also goes to my MSc Environmental Change 2012/2013, course mates for their love and support throughout the course; they were like a great family to me. Special mention is made of Miss Joyce Klu whose timely benevolence saved my withdrawal from the course, I am forever grateful. Also deserving special mention are Mr. Festus Asaaga, Ernest Kusi and Gonzalo Griebenow for their love, care and support during my studies in Oxford.

I also thank The Ghana Education Trust Fund (GETFund) for sponsoring me in the programme. And to the Green Templeton College, University of Oxford, for providing the conducive international environment during my studies and also, for sponsoring part of my fieldwork in Ghana for data collection.

And finally to my one and only 'better-half' who supported me all through, I will forever cherish you Mrs. Vida Appiah. To all who in diverse ways contributed to the success of this project, especially, friends we met at Assin-Foso in the Central region of Ghana, especially Mr. Alex of CCA and Police Officer Bosompem, I say God richly bless you all.

TABLE OF CONTENTS

LIST OF FIGURES

LIST OF TABLES

ABBREVIATIONS

FAO:	Food and Agriculture Organization
KCA:	Kakum Conservation Area
NDVI:	Normalized Differencing Vegetation Index
PCA:	Principal Component Analysis
GIS:	Geographical Information Systems
USGS:	United States Geological Survey
UTM:	Universal Transverse Mercator
DN:	Digital Numbers
DOS:	Dark Object Subtraction
ISODATA:	Iterative Self-Organizing Data Analysis Technigue
PIF:	Pseudo Invariant Features
FLAASH:	Fast Line-in-sight Atmospheric Analysis of Spectral Hypercubes
QUAC:	QUick Atmospheric Correction

CHAPTER ONE

INTRODUCTION AND THE STUDY AREA.

1.1 Introduction

Tropical forests provide vital ecosystem services and resources such as timber, medicinal plants, livelihood for their sustainable use, protection of vital watersheds, and also serve as a vital habitat for a large number of important fauna and flora, of high scientific value, without which they will go extinct. Malhi et al. (2010) points out, "tropical forests have a major influence on global patterns of biodiversity, ecosystem ecology, productivity and biogeochemical cycles, but they remain understudied". According to FAO (2005) we are losing about 50,000 plant and animal species as a result of depletion of tropical forests.

Ghana's high-biomass tropical rainforest is in a critical state as it continues to decline at an alarming rate of 2.2% yearly (FAO, 2010). Its service of supporting diversity of wildlife and provision of important products to local communities is seriously threatened. Essentially, rather than serving as a net carbon 'sink', it is becoming a carbon 'source' instead- majorly due to deforestation. Gibbs et al. (2007) averred that a majority of atmospheric carbon is sequestered in tropical forests from the aboveground tissues (e.g. trees) with secondary stocks lodged in soils and coarse woody debris.

One technology which offers considerable promise for monitoring land cover change is satellite remote sensing. This observation technology provides globally consistent, repetitive measurements of earth surface conditions relevant to climatology, hydrology, oceanography and land cover monitoring. One mission in particular, the Landsat Series begun in 1972, was designed and continues to operate with the objective of tracking changes in land cover conditions (Masek et al., 2000). The high spatial resolution and regular revisit times of the

Landsat mission are well suited to studies of national, regional and global land cover change. Rather than simply showing the gross change over a long period, these satellite time series can record the variability of land cover dynamics in space and time, permitting rigorous analyses.

One way of assessing land cover land use change using remote sensing and GIS is by way of Change Detection. This approach refers to the identification and location of changes in the state of an object or phenomenon through the examination of the changes in radiance values between sets of multi-temporal satellite images (Wang, 1993). The basic premises of remote sensing change detection are that changes in land cover results in changes in radiance values, and such changes from land cover are larger when compared to radiance changes caused by other factors (Mas, 1999). Change detection is also used as an evaluation tool for management practices, since changes to the environment can also reflect how the land has been managed (Brothers and Fish, 1978). To detect land cover change, a comparison of two or more satellite images acquired at different times can be used to evaluate the temporal or spectral reflectance differences that have occurred between them (Lunetta and Elvidge, 1998).

This study therefore sought to evaluate the land cover changes that have occurred in KCA over the past three decades using the integration of remote sensing and GIS applications.

1.2 Research question

What are the trajectories of land use changes in the Kakum forest and surrounding landscape?

1.3 Primary aims & specific objectives

This study aims to evaluate the land cover dynamics that had taken place in the Kakum forest area over the past three decades as a result of the changes in land use. The specific objectives of the project however will include:

(1) To classify available satellite images of the Kakum forest and use the classification maps to identify the trends of change in land cover type.

(2) To analyze and map land cover change trajectories in the Kakum forest ecosystem and the surrounding landscape.

(3) To identify areas of the Kakum forest landscape that had undergone significant land cover changes.

(4) To evaluate drivers of land use changes in the Kakum forest and the surrounding landscape.

1.4 Study Area:

1.4.1 Overview

Ghana has four distinct geographical regions. The Low plains stretch across the southern part of the country. To the north of these low plains lie three regions – the Ashanti Uplands, the Akwapim-Togo Ranges and the Volta Basin. The High plains, which is the fourth region, occupy the northern and northwestern sector of the country.

The Kakum tropical rainforest, which forms the study area for this project falls within the Ashanti Uplands, the Akwapim-Togo Ranges and the Volta Basin and contains remnants of Ghana's tropical rainforest belt. This is broken by heavily forested hills, many streams and rivers. It extends, northward from the shore near the Cote d'Ivoire frontier, where most of the country's cocoa, minerals and timber are produced.

The Kakum tropical rainforest, which forms the study area for this project falls within the Ashanti Uplands, the Akwapim-Togo Ranges and the Volta Basin and contains remnants of Ghana's tropical rainforest belt. This is broken by heavily forested hills, many streams and rivers. It extends, northward from the shore near the Cote d'Ivoire frontier, where most of the country's cocoa, minerals and timber are produced.

The Kakum forest consists of the Kakum National Park in the southern portion and the Assin-Attandanso resource reserves, these lie within latitudes 5°20′ and 5°40′ north and longitudes 1°30′ and 1°51′ west, resulting in a block of moist-evergreen forest approximately 366km^2, and together known as the Kakum Conservation Area (KCA) (Fig. 1.1). The KCA was gazetted in 1992 and falls within the jurisdiction of the Twifo Heman Lower Denkyira, Assin South, Assin North and Abura Asebu Kwamankese Districts. The mean annual rainfall in the area is between 1,500 and 1,800mm a year. This tends to fall in two peak seasons, the major rains falling from May to July and the minor rains falling from September to December. The dry season extends from January through to April. During the year, the temperature varies between 10°C and 32°C, while the average humidity is about 85%. The vegetation of the area is typically a moist evergreen forest type. There are a number of small rivers and streams that drain south-eastwards towards the sea, westwards and northwards into the Pra River and eastwards into other more minor rivers. The Kakum River serves as a source for much of the water supply for the city of Cape Coast.

1.4.2 Administrative Characteristics

The KCA is located in the administrative boundaries of three districts, namely Komenda Edina Eguafo Abirim District, Twifo Heman Lower Denkyira District, and Assin North

District. Official records of the 2000 population census and the Wildlife Division of the Forestry Commission of Ghana indicate that the area contains about 400 fringe communities and a total population of about 93,562.

In terms of forest and park management, the district assemblies are only responsible for creating awareness on activities such as poaching, bush burning, etc., which threatens adjoining forests and parks within their jurisdiction. All other forest management activities are left in the hands of the Wildlife Division and other appropriate state authorities.

1.4.3 Major Land Uses around the KCA

Major land uses in the KCA include farmlands and village settlements, with both subsistence and commercial agriculture taken prime place. Cash crops that are commonly cultivated in the area include cocoa, oil palm and citrus. All these land uses mainly occur outside the protected forests of the Kakum National Park and the Attandanso forests.

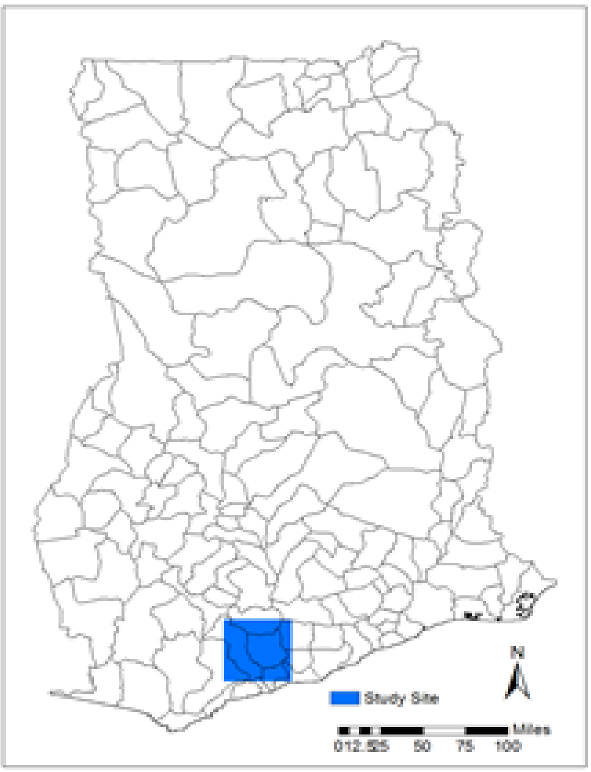

Figure 1.1 Map of Ghana showing KCA

Figure 1.2 Area Extent of the KCA

1.5 Layout of the dissertation.

Apart from chapter one, this dissertation consists of five more chapters. Chapter two gives an overview of the datasets used in this study. It also highlights some of the significant image pre-processing operations that were undertaken to make the data “ready” for the analytical stages. Chapter three presents the results and a discussion of the first objective of this study (i.e. an attempt to detect areas of possible land cover changes within the study area).

Chapter four addresses the second objective. It presents the results and the discussion of the findings of NDVI image differencing that was used to discern the land cover change trajectories that had occurred in the area. In chapter five, results of classification of the satellite images are presented. A discussion into the trends in land cover changes in each land cover type is also presented in this chapter. Finally, chapter six outlines the general conclusions that were drawn from this study and presents some of the recommendations for further research.

CHAPTER TWO

LAND COVER CHANGE DETECTION: MATERIALS AND METHODOLOGY REVIEW

2.1. Introduction.

Ecosystems are continuously changing, where change is defined as “an alteration of the surface component of vegetation cover”(Milne, 1988). The rate of change can either be dramatic and/or abrupt, as exemplified by fire, or subtle and/or gradual, such as biomass accumulation. Change can therefore be seen as a categorical variable (class) or in a continuum. Authors generally distinguish between land-cover conversions i.e. the complete replacement of one cover type from another, and land-cover modification, i.e. more subtle changes that affect the character of the land cover without changing its overall classification (Coppin et al, 2004).

From a conceptual perspective, land cover change detection permits the identification of long-term trends in time and space and the formulation of policy in anticipation of problems that accompany changes in land use. Timely and accurate change detection of the Earth’s surface features is extremely important for understanding relationships and interactions between human and natural phenomena in order to promote better decision making. Remote sensing data sources have been extensively used for change detection in recent decades. In remote sensing context, change detection has been defined as the identification and location of changes in radiance values between sets of multi-temporal images (Wang, 1993).

A number of land cover change detection techniques are currently in use in the field of remote sensing. Luneta and Elvidge (1999), groups these techniques into two main categories: (1) post classification comparison techniques and (2) enhancement change detection techniques. Post-classification techniques involve the production and subsequent comparison of spectral classifications for the same area at two or more different periods while enhancement techniques involve mathematical combination and analysis of images from different dates (Richards, 1993).

Other authors have attached definitions that vary in complexity and, to a certain extent, in coverage to these categories. Malila (1980) recognized the categories as change measurement (stratification) methods versus classification approaches. Pilon et al (1987) amplified the description of the change measurement category to “enhancement approaches involving mathematical combinations of multi-date imagery which, when displayed as a composite image, show changes in unique colours”. Singh (1989) changed the focus slightly by centring the definitions more on temporal scale: simultaneous analysis of multi-temporal data versus comparative analysis of independently produced classifications for different dates.

Whichever method one chooses to use, both the two approaches have advantages and disadvantages. The first approach (comparative analysis of independently produced classifications from different dates) has several sources of uncertainty. Aspinall and Hill (1997) emphasizes two of them: (1) misregistration of the polygon boundaries (location inaccuracy) in the direct classification and, therefore, the presence of border pixels with false positive and negative changes and (2) problems derived from classification errors: false positive change can be recorded when no change has occurred because a polygon in one or both of the two maps is misclassified or false negative changes, when no change is identified but a change has taken place.

In the case of the second approach (simultaneous analysis of multi-temporal data), several procedures have been developed, such as image differencing, vegetation index differencing, principal components analysis and change vector analysis (Fung and LeDrew, 1987; Lambin and Strahler, 1994). In these procedures, the basic premise is that changes in land cover must result in changes in reflectance values, which must be larger than those caused by other factors such as differences in atmospheric conditions, sun angle, soil moisture or precise sensor calibration. The impacts of some of these factors may be partially reduced by selecting image acquisition dates as close as possible for different years used (Serra et al, 2003). Nevertheless, there are some problems related to this second approach: (1) most of these procedures provide little information about the specific nature of land cover change, (2) the threshold technique used to differentiate change from no-change areas is usually not clear and, (3) the misregistration between metadata images.

In the following sections the data sets used in this study are described and a review of the methods used is presented.

2.2. Data set description.

The data sets that were used in this study included satellite images, GIS databases and GPS ground control points. All pre-processing and processing activities were done using the ENVI 5.0 and ERDAS IMAGINE image processing softwares.

2.2.1. Satellite Images.

KCA covers an area of approximately 366 km2, which only required a single image scene with a single path and row for the Landsat TM and ETM+ images. The attributes of the images used in this study are presented in table 2.1.

All the images were acquired from the U.S. Geological Survey (USGS) website: http://landsat.usgs.gov/

Table 2.1. Description of the satellite images used in this study.

Image Acquisition Date	Landsat Sensor	Spatial Resolution	Others
29/12/1986	TM 5	30 meters	Path/Row: 194/56 S/E:
01/01/1991	TM 4	30 meters	Path/Row: 194/56 S/E: 44.68
02/04/2001	ETM+ 7	30 meters	Path/Row: 194/56 S/E: 60.66
27/04/2013	ETM+ 7	30 meters	Path/Row: 194/56 S/E: 64.05

All the images were taken in the dry months of December, January and April. This ensured that errors arising from seasonal differences (vegetation phenology) were minimized. The major consideration for selecting these images over others was to have a consistent ten year interval between them, with exception of the 1986 image, which was the appropriate earliest image.

2.3. Image pre-processing.

The primary challenge in deriving accurate natural ecosystem change information is representative of the standard remote sensing problem: maximizing of the signal-to-noise ratio (Coppin et al, 2004). Inherent noise will affect the change detection capabilities of a system or even create unreal change phenomena. The causes of such unreal changes can be, among others, differences in atmospheric absorption and scattering due to variations in water vapour and aerosol concentrations in the atmosphere at disparate moments in time, temporal variations in the solar zenith and/or azimuth angles, and sensor calibration inconsistencies for separate images (Coppin et al, 2004).

Pre-processing of satellite sensor images prior to actual change detection is essential and has as its unique goals the establishment of a more direct linkage between the data and biophysical phenomena, the removal of data acquisition errors and image noise, and the masking of contaminated (e.g. clouds) scene fragments. Typically, image pre-processing consists of a series of sequential operations such as calibration to radiance or at satellite reflectance, atmospheric correction or normalization, image registration, geometric correction, mosaicking, sub-setting and masking.

A series of the significant pre-processing operations undertaken in this study are reviewed in the following sections.

2.3.1. De-striping.

De-striping refers to the application of algorithms to adjust incorrect brightness values to values thought to be near correct values (Campbell, 2002). Landsat MSS data sometimes exhibit a kind of radiometric error known as sixth line striping, caused by small differences in the sensitivities of detectors within the sensor. Within a given band such differences appear on the images as horizontal banding, or “striping”, because individual scan lines exhibit unusually brighter or darker brightness values that contrast noticeably with the background brightness of the “normal” detectors (Mather, 1999). Landsat TM data can suffer from a similar banding problem. However, the Landsat TM imagery is recorded in 16 detectors per band for all non-thermal bands and 4 detectors for the thermal band (Lillesand and Kiefer, 1996) and hence the problem is minimized. In relatively newer sensors such as ETM+, the problem has largely been eliminated due to better satellite stability and the presence of on-board calibration systems (Mather, 1999).

Some of the arguments that have been put forward for de-striping of Landsat MSS imagery include: the improvement in the visual appearance and interpretability of the image and equal pixel values in the image are more likely to represent areas of equal ground leaving radiance, other things being equal. However, other research (Campbell and Liu, 1995) found that de-striping the image has little impact on the character of the data.

A variety of de-striping algorithms have been devised. All of these identify the values generated by the defective detectors by searching for lines that are noticeably brighter or darker than the lines of the remainder of the scene. Among these algorithms are simple along-line convolution, high-pass filtering and forward and reverse principal component transformations (Crippen, 1989), histogram normalization for each scan-lines associated with each sensor (Mather, 1999) and image editing in the frequency domain (Srinivasan et al, 1988).

After visual inspection of the images used in this study, it was decided that none of the images required de-striping.

2.3.2. Conversion of Digital Numbers to Radiance Values.

Calculation of radiance values is a fundamental step in putting image data from multiple sensors and platforms into a common radiometric scale. This is an essential step in land cover change detection studies based on multi-temporal images. In this study two sets of equations were used to convert digital numbers (DN) to radiance values.

For Landsat TM and ETM+ images, the following equation was used for converting DN into radiance values (Markham and Chander, 2003):

$$L\lambda = \left[\frac{L\max\lambda - L\min\lambda}{Qcal\max}\right]Qcal + L\min\lambda$$ .... Equations (1).

Where:

$L\lambda$ = Spectral radiance at the sensor's aperture in Watts/(m2*sr*µm)

Qcal = the quantized calibrated pixel value in Digital Number (DN).

Qcalmin = the minimum quantized calibrated pixel value (DN=0) corresponding to $Lmin\lambda$.

Qcalma x= the maximum quantized calibrated pixel value (DN=255) corresponding to $Lmax\lambda$.

$Lmin\lambda$ = the spectral radiance that is scaled to Qcalmin in Watts/(m2*sr*µm)

$Lmax\lambda$ = the spectral radiance that is scaled to Qcalmax in Watts/(m2*sr*µm)

All these values were obtained from the image metadata files.

Finally, when comparing two or more images, it is advisable to do some normalization to reduce between-scene variability that is due to effects like the sun angle and distance between the sun and the earth (Pickup et al, 1993). For relatively clear Landsat scenes, converting spectral radiance values (from equation 1) to planetary reflectance (equation 2) is commonly suggested, taking into account sun angle and distance between the sun and the earth (Markham and Barker, 1986).

The equation is as follows:

$$Pp = \frac{\prod * L\lambda * d^2}{Esun\lambda * Cos\theta s}$$ ………………………… Equation (2)

Where:

Pp = Unitless planetary reflectance

$L\lambda$ = Spectral radiance at the sensor's aperture.

d = Earth-sun distance in astronomical units.

$Esun\lambda$ = Mean solar exoatmospheric irradiances

θs = Solar zenith angle in degrees.

However, in this study, the transformation of radiance values to spectral reflectance using equation 3 was avoided after it became apparent that the image quality was degraded when these calculations were attempted. Therefore, in order to correct for between-scene variability, another method was used (i.e. the atmospheric correction method).

2.3.3. Atmospheric Correction.

Usually, the presence of atmosphere between the ground and the satellites means that a pixel value in remotely sensed image is unlikely to truly represent the ground leaving radiance. Radiation from the earth's surface interacts through absorption and scattering by the atmosphere before it reaches the sensor. The amount of atmospheric interaction/distortion is wavelength dependent, with shorter wavelengths experiencing more scattering than longer wavelengths (Sabins, 1997).

In order to extract quantitative information and compare satellite images, atmospheric correction is considered a necessary step. There is relatively a long list of atmospheric correction methods of Landsat imagery. Liang et al (2001) classified these methods into the following groups: invariant-object, histogram matching, dark object, and the contrast reduction. If sufficient information is known about the atmosphere at the time of image acquisition, then atmospheric correction can be performed through the use of models such as LOWTRAN/MODTRAN and 6S (Chavez, 1996) and QUAC application (ENVI, 2012) However, in this study, such detailed meteorological information was lacking and hence a simplistic atmospheric correction method that exploited data contained in the image itself was used.

The dark pixel subtraction (DOS) was used as a direct and effective method for correcting atmospheric effects. The principle behind the dark object subtraction also known as the histogram minimum method (HMM) is that some dark objects (e.g. deep water or dark dense vegetation) in the image will have zero or near zero reflectances in certain wavebands. However, due to atmospheric scattering, the minimum values of these dark pixels are usually not zero, but some larger value (Campbell, 2002). These minimum values for each band are then assumed to represent the contribution of atmospheric scattering. Therefore, if the minimum is subtracted for each band, the lowest value of each band is set to zero, assuming zero to be the correct signature for dark objects in the absence of atmospheric scattering.

In this study, water features were selected and an area of interest (AOI) identified and the mean values of each band in these areas of interest calculated. These mean values were then used in the dark object subtraction procedure. However, it is important to note that care should be taken when choosing the dark objects as some of these objects are not "dark enough" and could actually have reflectance values that are not zero e.g. water containing sediments. This was guarded against in this study by inspecting various dark objects and only choosing those that had the minimum mean values in most of the bands for the atmospheric correction procedure. The atmospheric correction procedure was executed using the ENVI 5.0 image processing software (ENVI, 2012).

2.3.4. Geometric Correction.

Geometric correction addresses the errors in the relative positions of pixels. The images used in this study were acquired already systematically corrected for sensor geometry and terrain variations to Level 1G by the U.S. Geological Survey (USGS). Systematic correction refers to the nature of geometric correction applied to images by employing a correction algorithm that models the spacecraft and sensor, using data generated by onboard computers during imaging events (Landsat 7, 2003). However, it is worth noting that in that correction there were no ground control points (GCPs) or relief models applied to obtain absolute geodetic accuracy (Landsat 7, 2003) and hence the algorithms used could have residual errors. To ensure that there were minimal errors, the images were visually inspected through "swipe" functionality in ENVI and it was concluded that the correction undertaken by the USGS was acceptable as all the images showed perfect registration to each other.

2.4. Image Processing.

The previous section (Section 2.3) reviewed the image pre-processing operations that were undertaken to make the images "ready" for the essential image analysis considered necessary in achieving the objectives of this study. In this section, a review of the image analysis operations employed in this study is presented.

2.4.1. Principal Components Analysis.

Principal components analysis (PCA) also referred to as Karhunen-Loeve (K-L) transformation is a commonly used statistical method for many aspects of remote sensing image analysis, including estimation of the underlying dimensions of remotely sensed data and data enhancement for land cover change detection (Fung and LeDrew, 1987). PCA is based on the notion that most remotely sensed images exhibit high inter-band correlations.

The theory of PCA is that two normally distributed bands of image data will form an elliptical shape if the bands are correlated and a circle if they are not, when data are plotted in a scattergram. The line that corresponds to the major axis of the ellipse becomes the first principal component and it represents the widest transect of the ellipse and measures the largest variation within the data (Mather, 1999). The eigenvalue of the principal components (PC) is the length of the transect measured in units of variance and the eigenvector of the PC are the coordinates defining its direction. The second PC is the line through the ellipse that is orthogonal to PC1 and describes the largest variance in the data that is not already described by PC1. In an n-dimensional spectral space, a hyper-ellipsoid shape is created when there are more than 3 dimensions to the data set, and each successive PC beyond PC2 will still be perpendicular to all other PC's and will account for a decreasing amount of the total variation in the data (ENVI, 2012).

In operational terms, the principal component transformation can be divided into three steps (Richards, 1984):

(i) The images are first registered to form a single multi-band image containing all the bands from each date.

(ii) Next follows the derivation of the variance-covariance matrix, which is used to determine the eigenvectors (the coefficient to be applied to each band in order to weight its inclusion in the new image)

(iii) The PCA then identifies the optimum linear combination of all the bands that can account for the image to create a new image. The Linear combination is in the form:

$PC1= C_1X_1+C_2X_2+C_3X_3+C_4X_4$……………. Equation (3)

Where:

X_1=the pixel values in band 1.

C_1= the coefficient applied to band 1 (Eigenvectors).

PC= the principal component.

The maximum number of principal components (PCs) that can be produced from one image is equal to the number of bands in the image and each PC will be statistically independent from all other PCs.

PCA has been used in change detection studies since it enhances regions of change in an image because of the high correlation that exists between data for regions of little or no change and low correlation between data for regions of significant change. Areas of little or no change will therefore be mapped to the first PC and areas of change will be mapped to higher order PCs (Siljerstron and Lopez, 1995).

2.4.2. Normalized Difference Vegetation Index (NDVI) Computation.

Vegetation indices (VIs) based upon digital brightness, have been extensively used to study vegetation biomass or vigour (Tucker, 1979; 1986). The indices are based on the premise that chlorophyll in actively growing vegetation is a strong absorber of red radiation, and the cell-wall structure of healthy leaves strongly reflects Near Infrared (NIR) radiation. Therefore, greater photosynthetic activity will result in lower reflectance in the red band and higher reflectance in the NIR. It is for this reason that the red and the NIR regions of the electromagnetic spectrum are primary bands utilized in remote sensing of vegetation. By combining these two spectral regions in a ratio or difference, the NDVI, the sensitivity to photosynthetic activity is enhanced. While a variety of vegetation indices have been used over the past decades, the NDVI is the most commonly applied index:

$$NDVI = \frac{NIR - RED}{NIR + RED}$$ ………………………… Equation (4).

By normalizing the difference between the channel values, NDVI values are scaled to lie in the range between –1 to +1. High positive values of NDVI correspond to dense vegetation cover whereas negative values are usually associated with bare soils, snow, clouds or non-vegetated surfaces (Oindo and Skidmore, 2000).

In this study, the NDVI values were calculated using the ENVI Spectral function using the following equations:

For Landsat TM and ETM+:

$$NDVI = \frac{Band4 - Band3}{Band4 + Band3}$$ …………………………….. Equation (5).

2.4.3. Classification.

The classification process has been described as consisting of two stages (Mather, 1999). The first is the recognition of categories of real-world objects. In the context of remote sensing of land surface these categories could include, for example, woodlands, water bodies, grasslands, and other land cover types depending on the geographical scale and nature of the study. The second stage in the classification process is the labelling of the entities (normally pixels) to be classified. The process of classification often requires the user to: (1) determine a prior the number and nature of the categories in terms of which the land cover is to be described and, (2) assign numerical levels to the pixels on the basis of their properties using a decision making procedure, usually termed a decision rule or classification rule. There are three distinct kinds of classification that are in use in the field of remote sensing: unsupervised, supervised and hybrid classification. A brief review of the classification methods used in this study is presented below.

2.4.3.1. Unsupervised Classification.

It is defined as the identification of natural groups, or structures, within multi-spectral data. The most widely used algorithm for performing unsupervised classification is the Iterative Self-Organizing Data Analysis Technique (ISODATA). ISODATA produces results that are often considered to be superior to those derived from basic minimum distance classifiers (Campbell, 1996). ISODATA requires the user to input the maximum number of classes desired, the maximum number of iterations for the algorithm, and the threshold value for the average inter-centre Euclidean distance. It then assigns pixels in an image to one of the N-clusters in multidimensional feature space and calculates the mean value for each spectral band. Furthermore, it calculates the spectral distance between each candidate pixel and the mean for the cluster it is currently assigned to. If that pixel's value is closer to the mean of another cluster, then it is reassigned to that other cluster. The pixel reassignment and calculation of all cluster means process, is repeated until the total number of iterations specified has been completed (ENVI, 2012).

2.4.3.2. Supervised classification.

Supervised classification is more closely controlled than an unsupervised classification. It has been defined informally as the process of using samples of known identity (i.e. pixels already assigned to informational classes) to classify pixels of unknown identity (i.e. to assign unclassified pixels to one of the several informational classes) (Campbell, 2002). Knowledge of the data, the classes desired, and the algorithm to be used is required before training is done. By identifying patterns in the imagery, the computer system is trained to identify pixels with similar characteristics. There are a several algorithms for performing supervised classification, but the most commonly used method is the maximum likelihood classifier. It is also considered to be the most accurate of the classifiers compared to other algorithms (ENVI, 2012).

2.4.3.3. Hybrid Classification.

A hybrid classification also referred to as guided clustering, involves a combination of both unsupervised and supervised classification. An unsupervised classification is initially performed to identify spectral differences within the data and then a supervised classification is performed using areas of the unsupervised classification as training data in addition to ancillary ground-truth. Among the advantages of this approach is its ability to help the analyst to identify the various spectral subclasses representing information class "automatically" through clustering. At the same time the process of labelling the spectral clusters is straight forward because these are developed for one information class at a time. Hybrid classifiers have also been observed to be of particular value in the analysis where there is complex variability in the spectral response patterns of individual cover types, a condition that is quite common in vegetation mapping (Lillesand and Kiefer, 2000).

2.5. Accuracy Assessment.

Accuracy assessment allows a researcher to compare certain pixel values in the thematic raster layer (original image) to the reference pixels, for which the class is known. This is an organized way of comparing the classification with ground-truth data, a previously tested map, aerial photos, or other data of the study area. Accuracy assessment is therefore important for understanding the developed results and employing these results for decision-making.

The most common accuracy assessment method is the preparation of a classification error matrix (or confusion matrix). Error matrix compares, on a category-by-category basis, the relationship between known pixel reference data and corresponding results of an automated classification. The most common elements of the error matrix accuracy assessment include overall accuracy, producer's accuracy, user's accuracy and kappa coefficient (Lillesand and Kiefer, 2000).

CHAPTER THREE

DETECTION OF AREAS OF POSSIBLE LAND COVER CHANGES IN THE KCA.

3.1. Introduction.

Temporal changes in landscape composition and structure result from biological, physical and human influences. Knowledge of these changes and their driving processes provides insight into regional landscape dynamics. Several methods have been used in the field of remote sensing to study these dynamics in landscapes. The choice of what method to use in such studies is highly subjective and is linked to the objectives of that particular study. In the present study, the principal component analysis was adopted, for the reason that it has been shown to perform better in land cover change detection studies in areas where large proportions belong to no change (Richards, 1984), as is assumed to be the case in most tropical forest ecosystems and areas of significant change clearly noticeable.

Principal components analysis (PCA) is a multivariate analysis technique used for data reduction. It concentrates information pertaining to statistically minor modifications in the state of the natural ecosystems (minor contrasted to the entirety of the image) in orthogonal components, producing uncorrelated differences. PCA has been used in land cover change detection studies due to the fact that it enhances regions of change in an image because of high correlation that exists between data for regions of little or no change and low correlation between data for regions of significant changes. Therefore, areas of little or no change will be mapped to the first principal component (PC) and areas of change will be mapped to the higher order PCs (Siljerston and Lopez, 1995).

Several studies have used PCA in land cover change detection with varying degrees of success. For example, Richards (1984) applied normal PCA approach to two-date MSS imagery to monitor bush-fire damage and vegetation re-growth over extensive areas in Australia. He found out that, provided the major portion of the variance in the multi-temporal sequence was associated with correlated land cover, areas of localized change were enhanced in some of the lower components, particularly PCs three and four. Ingebritsen and Lyon (1985) did exactly the same thing to detect and monitor vegetation changes around a large open-pit uranium mine in Washington and wetland area in Nevada. Under the assumption that the two original images both had an intrinsic dimensionality of two, they found four meaningful PCs in their study. These included PCs representing stable brightness, stable greenness, change in albedo and change in greenness. The latter component proved to be well related to changes in vegetation cover and insensitive to variations in slope and aspect.

Two approaches to PCA are currently in use in remote sensing change detection studies: (1) independent transformation PCA and (2) merged data transformation. Independent transformations involve undertaking PCA on each single image and thereafter comparing their results. Merged data transform on the other hand involves superimposing images before hand and then performing PCA of the merged data (Estes et al, 1982). Apart from these two approaches, during implementation of PCA, one can choose to either use the entire bands of the image or a selection of bands. Studies by Coppin and Bauer (1994) found that the use of selected bands was more successful in discerning areas of change in their study of temperate forest cover in the north-central USA. They particularly found the second principal component of vegetation index band pairs to be an excellent indicator of change. Kwarteng and Chavez (1998) used similar selective PCA approach to successfully detect and map surface changes dealing with urban development, vegetation growth and coastal and sand sheet surface differences.

It is worth noting that the exact nature of the principal components derived from multi-temporal datasets in land cover change detection studies are still difficult to ascertain. Suggestions that have been made that could help in overcoming this problem include a thorough examination of the eigenstructure of the data and visual inspection of the combined images. Another way is to look for the presence of areas with significant departures from the grey scale in the later PCs (Fung and LeDrew, 1987). Finally, to avoid drawing the wrong conclusions, knowledge of the study area is desirable.

3.2. Methodology

The merged data PCA approach was adopted whereby pairs of images were first merged together using the layer-stack function of ENVI 5.0 (IDL 8.2) image processing software. However, not all the bands of each image were used in the PCA operation, but a selection of specific bands 2, 3 and 4 for the Landsat TM and ETM+ images. The reason for this choice of bands was the fact that they are the bands used in characterization of vegetation activity, a principal focus of this study.

The principal components analysis was then performed on the merged images according to the procedures outlined in the ENVI users' guide (ENVI, 2012). The following sections present the results and discussions of the PCA operations.

3.3. Results

3.3.1. Principal Components Analysis of Multidate 1986 and 1991 Images.

A merged PCA of dates 1986 TM and 1991 TM image was performed to try to identify areas that had undergone significant land cover changes in the KCA. Bands 2, 3 and 4 from the TM images were utilized in the process.

Six principal components (PCs) were identified as shown in Figure 3.3. The eigenvectors and the eigenvalues of the PCA of the merged 1986 TM and 1991 TM images are given in Table 3.1 and 3.2 respectively.

Table 3.1 Eigenvectors (Loadings) for PCA of the Merged 1986 TM and 1991 TM images

Merged Bands	Original bands	PC1	PC2	PC3	PC4	PC5	PC6
1	TM2	0.04741	-0.06776	-0.12832	-0.68512	-0.27438	0.657278
2	TM3	0.034309	-0.0141	-0.17657	-0.68993	0.221171	-0.66523
3	TM4	0.37351	-0.88204	0.282742	0.012202	0.002577	-0.04888
4	ETM2	0.137209	-0.13672	-0.65037	0.187789	-0.6701	-0.23495
5	ETM3	0.075625	-0.19282	-0.66847	0.137494	0.651223	0.259331
6	ETM4	0.912425	0.401666	0.050771	0.016912	0.051678	0.02471

Table 3.2 Eigenvalues from the PCA of the Multidate 1986 and 1991 Images.

Eigenvalues	Percentage Variance (%)
44.26241	73.59
7.073412	4.25
4.644638	2.79
3.089724	1.86
0.578512	0. 35
0.496841	0.30

The first principal component (PC1) is very highly loaded in the red and green channels 1,2,4 and 5 and is responsible for 73.59% of the variance. The fact that this PC is highly loaded in the red and green channels can be inferred to mean that it is the PC that represents the overall brightness of the study area (Fung and LeDrew, 1987).

The second (PC2) and the fourth (PC3) components seem to express the differences between the two images as can be seen from the algebraic signs of their loadings. In these two PC's all the channels (apart from channel 1 in PC3) that are negatively loaded in one date are positively loaded in the other and vice-versa (Figure 3.1). Visual inspection of these PC's support the assertion that areas of land cover change seem to be mapped on these two PC's as there exists areas that have either heightened dark tones or elevated brightness, a phenomenon that has been associated with areas representing change in land cover change detection studies using principal component analysis (Byrne et al 1980; Fung and LeDrew, 1987). Note that PC2 is considered to be highlighting areas of change in the present study, since not all the bands were used but a selection of vegetation indices bands. Other studies have shown that this PC particularly maps areas of vegetation change when a selection of vegetation indices bands is used in PCA (Kwarteng and Chavez, 1998).

Principal component three (PC3) showed higher loadings in the infrared channels 3 and 6. This represents a summary of the multi-date infrared reflectance and can be inferred to symbolize the overall greenness of the study area. PC5 was much harder to interpret as it loadings did not have any inherent pattern and visual inspection too did not yield any significant patterns, though they could be interpreted to represent noise in the data.

Fig. 3.1: Result of Principal Component from Multidate 1986 and 1991 Image

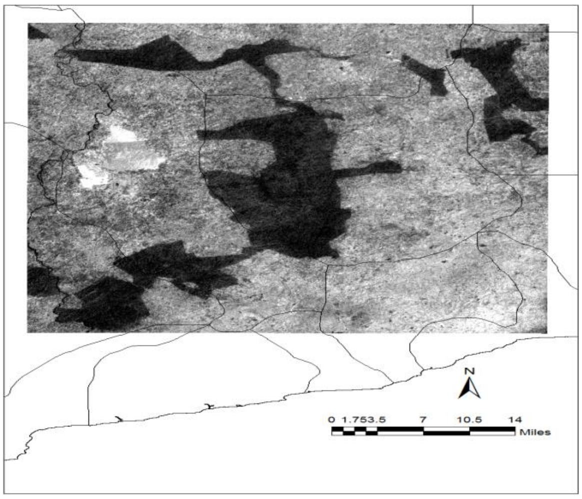

PC1

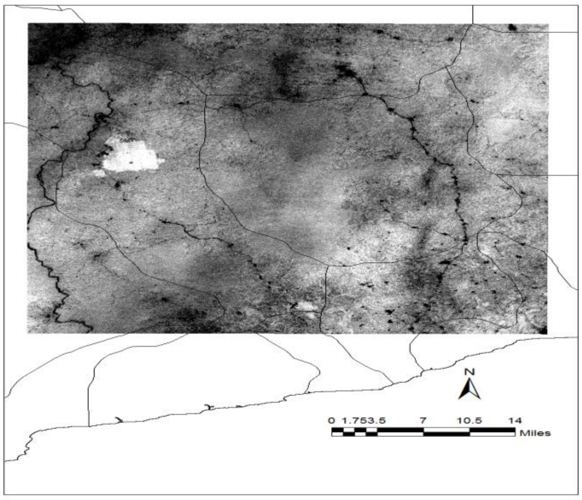

PC2

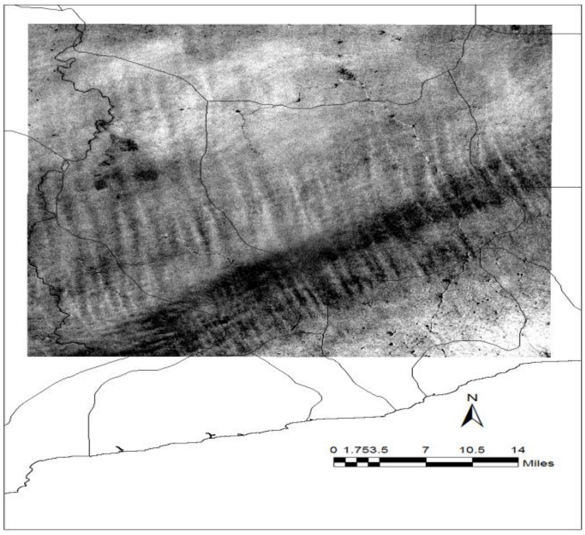

PC3

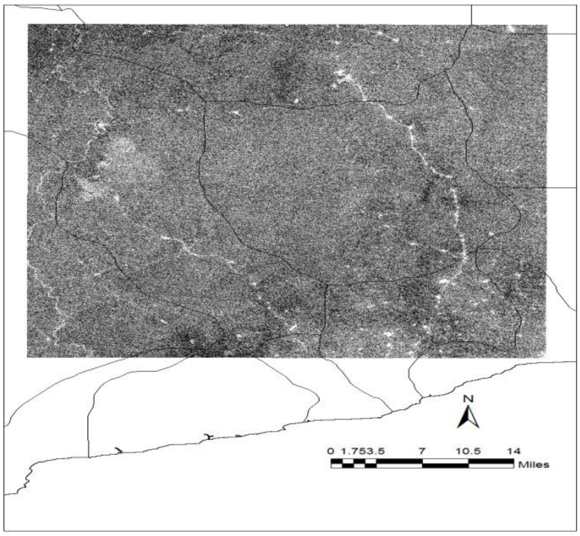

PC4

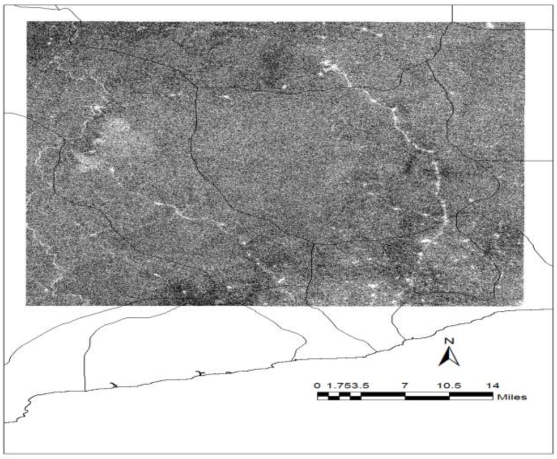

PC5

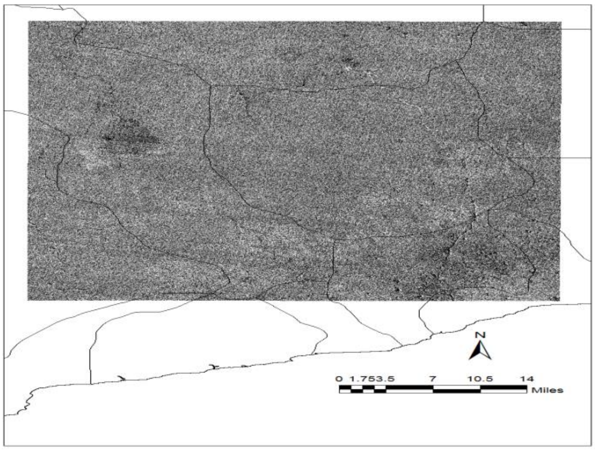

PC6

3.3.2. Principal Components Analysis of Merged 1991 and 2001 Image.

The merged 1991 TM and 2001 ETM+ image of the KCA was analyzed using PCA. In this analysis, a selection of bands (bands 2,3 and 4) was used from the two images. The resulting six principal components (PCs) are shown in figure 3.2. The resultant eigenvectors and eigenvalues are presented in table 3.3 and 3.4 respectively.

Looking at the eigenvectors of the various PCs, it is evident that PC1 has high positive loadings in the green and red channels 1,2,4 and 5. These high loadings in the green and red channels suggest that this PC mainly represents the general brightness of the vegetation conditions in the KCA. It also explains most of the variance (71.56 %) of the merged data set.

Table 3.3 Eigenvectors (Loadings) for PCA of the Merged 1991 TM and 2001 TM images

Merged Bands	PC1	PC2	PC3	PC4	PC5	PC6
1	0.041321	-0.0209	-0.12137	-0.68473	-0.10647	0.709182

2	0.028572	-0.00786	-0.05371	-0.71405	0.0233	-0.69701
3	0.197767	-0.19895	-0.94848	0.133875	-0.02793	-0.05464
4	0.702736	0.005961	0.176495	0.053051	-0.68433	-0.06208
5	0.678813	0.140727	0.084263	-0.02132	0.712444	0.065399
6	0.061143	-0.96958	0.210988	-0.00969	0.107036	0.010687

Table 3.4 The Eigenvalues from the PCA of the Multidate 1991 and 2001 Images.

Eigenvalues	Percentage Variance (%)
89.97142	71.56
29.07844	23.13
4.691731	3.73
1.417785	1.13
0.566711	0.45

Fig. 3.2: Result of Principal Component from Multidate 1991 and 2001 Image.

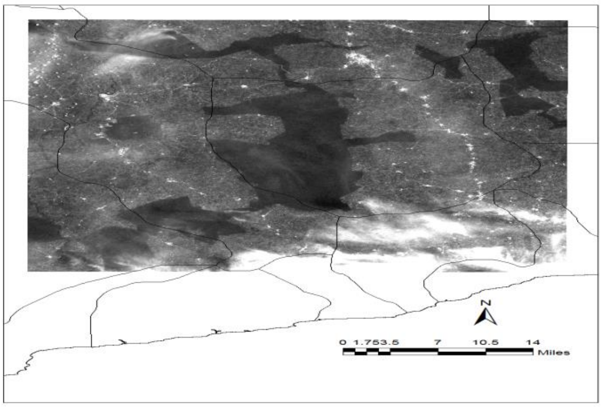

PC1

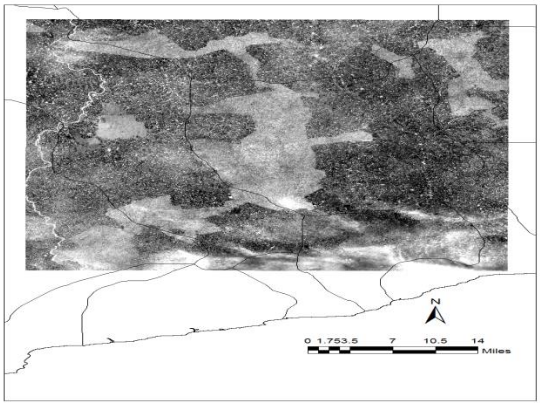

PC2

P

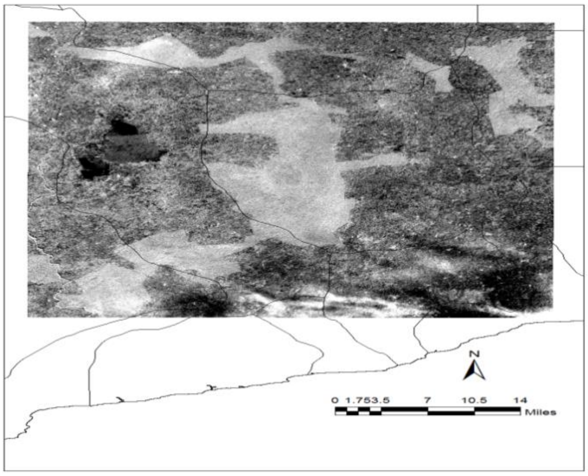

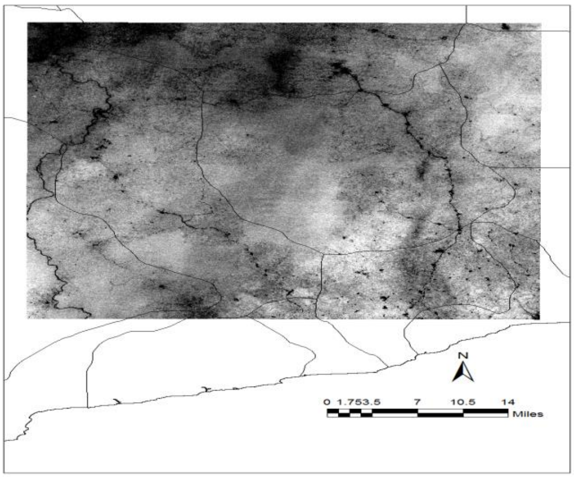

PC3

PC4

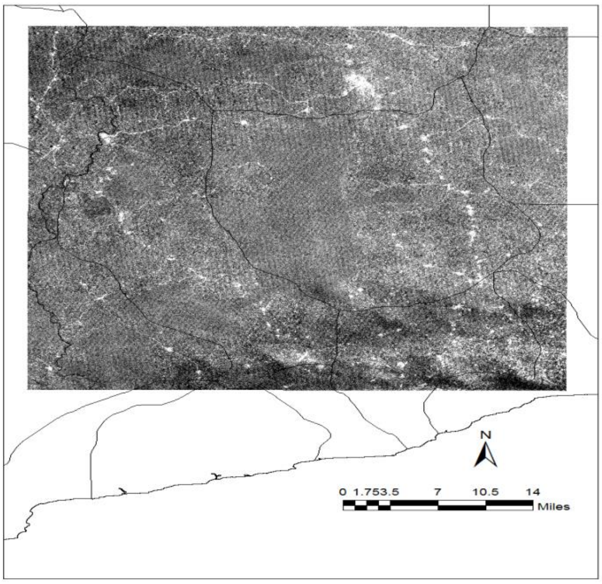

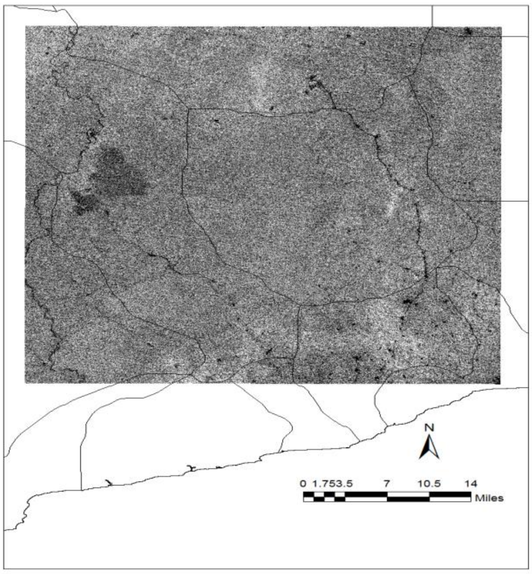

PC5

PC6

3.3.3. Principal Components Analysis of Merged 2001 and 2013 Image.

The resulting six principal components (PCs) are shown in figure 3.3. The resultant eigenvectors and eigenvalues are presented in table 3.5 and 3.6 respectively.

Looking at the eigenvectors of the various PCs, it is evident that PC1 has high positive loadings in the green and red channels 1,2,4 and 5. These high loadings in the green and red channels suggest that this PC mainly represent the general brightness of the vegetation conditions in Laikipia district. It also explains most of the variance (83.51 %) in the merged data set.

Table 3.5 Eigenvectors (Loadings) for PCA of the Merged 2001 ETM and 2013 ETM images

Merged Bands	PC1	PC2	PC3	PC4	PC5	PC6
1	0.044663	0.202062	-0.68954	-0.00842	0.189986	0.667497
2	0.043965	0.210068	-0.65434	0.131576	-0.16796	-0.69301
3	0.004953	-0.07126	-0.11065	-0.98605	-0.03532	-0.09546
4	0.697227	0.119315	0.094952	-0.02283	0.677143	-0.1777
5	0.654088	0.245787	0.102107	-0.01903	-0.68405	0.181768
6	0.286516	-0.91396	-0.25436	0.097162	-0.08941	0.021416

Table 3.6 The Eigenvalues from the PCA of the Multidate 2001 and 2013 Images.

Eigenvalues	Percentage Variance (%)
3171.552	83.51

361.4638	9.52
175.1787	4.61
84.95453	2.24
3.145506	0.08
1.346705	0.04

Fig. 3.3: Result of Principal Component from Multidate 2001 and 2013 Image.

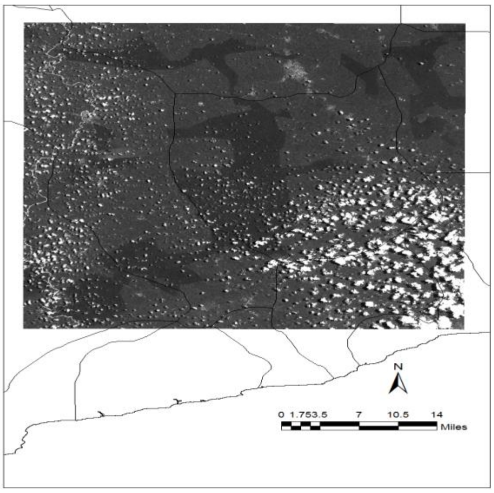

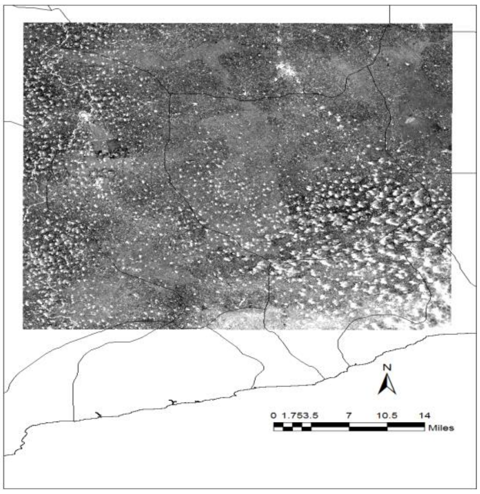

PC1 PC2

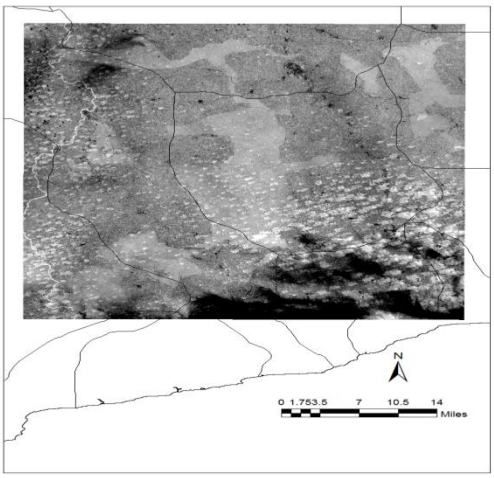

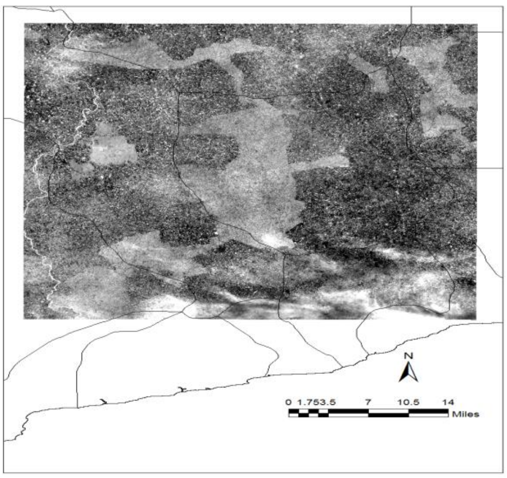

PC3 PC4

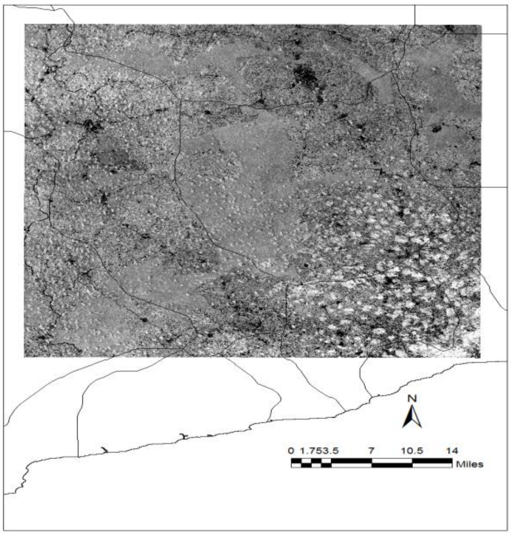

PC5

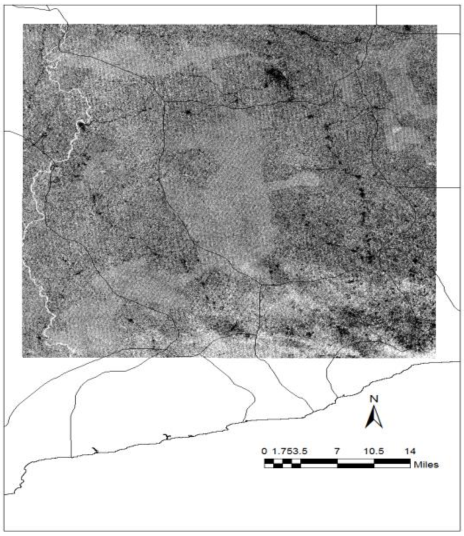

PC6

3.4. Discussions

The PCA of the three sets of merged data was able to detect areas that had experienced possible land cover changes in the KCA over the study period.

Starting with the results of the PCA of the merged data of 1986 and 1991 images, it was evident that a number of areas showed characteristics associated with land cover changes in specifically two principal components (PC2 and PC4). Both visual inspection and algebraic loading patterns of these two PCs proved crucial in making judgments that they were the PCs most likely representing areas of land cover change in the district.

Using the data collected during fieldwork coupled with the existing land use map (Figure 1.3), possible reasons for the observed areas of possible land cover change could be deduced. For example, the regions in the northwestern parts of the main protected forest (the Kakum-Attandanso forests) showed heightened brightness meaning some form of change had taken place in these areas. During fieldwork, it was noted that this area is currently under intensive cultivation agriculture. Therefore, the changes that appear to be detected by the results of the PCA in these areas could be linked to the farming activities that have been introduced in these areas leading to clearance of forests and other vegetation types to give way for cultivation lands.

Other regions that showed some elements of possible land cover changes include the areas around Kakum forest in the southeastern part of the area. It was established that this region has been and is still under communal cocoa agricultural activities. One possible explanation for the observed land cover changes in this area could be due to high cocoa and other cash crops price increases, incentivising farmers and especially landowners to open up more previously vegetated lands for agriculture.

Turning to the PCA results of the merged data of 1986 and 1991 images, more areas of possible land cover changes were discerned. PC2, PC3 and PC4 in particular seemed to highlight most of these areas. Ancillary data collected during fieldwork was used to try and infer the causes of the observed areas of possible land cover changes. The southwestern parts of the area were again highlighted in the results of the PCA of these two dates. As was explained earlier, this is a region that has been experiencing intensified cultivation agriculture from the ever growing number of immigrant cocoa-agricultural communities in the area. Therefore, it would be right to observe that the possible causes of the changes being depicted in the PCA results are due to the fluxes in land use activities (clearing of vegetation to give room to cultivate land) in this region.

3.5. Conclusion.

It is evident that the principal component analysis (PCA) of the merged data of the satellite images was able to detect areas that might have had some forms of land cover changes over the study period in the KCA. Most of these changes had links with the land use activities being practiced in the area (Figure1.1). Areas such as those that had undergone intensification of agriculture were highlighted as having experienced some form of land cover changes.

It can be concluded that the changes in land use activities in KCA outside the protected Kakum and Assin-Attandanso forests have had detectable changes in its land cover status. However, until further analyses are undertaken to ascertain the characteristics of these changes, it is hard at this stage to state the conclusive reasons for them. Nevertheless, the results prove that PCA is a quick and viable algorithm that can be used to detect areas of change in vast ecosystems such as the tropical forests. This can be of great importance in helping to identify areas to focus on during detailed studies in such vast ecosystems.

CHAPTER FOUR

DETERMINING LAND COVER CHANGE TRAJECTORIES IN THE KCA

4.1. Introduction

The principal components analysis discussed in chapter 3 acted as a general indicator of which areas in the KCA might have experienced land cover changes over the study period. However, from the PCA alone, it is hard to establish the characteristics/trajectories of these changes (i.e. whether they were increases in land cover or decreases in land cover). Therefore, to ascertain these trajectories, the univariate NDVI image differencing technique was adopted.

The univariate image differencing has been suggested to be the most widely used change detection algorithm (Coppin et al, 2004). It involves subtracting one date of original or transformed (e.g. vegetation indices) imagery from a second date that has been precisely registered to the first. With "perfect" data this would result in a dataset in which positive and negative values represent areas of change and zero values represent no change.

Several studies have used this algorithm in change detection with varied success. For example, Lyon et al (1998) implemented NDVI differencing and found it to be a better vegetation change detection technique for monitoring deforestation and loss of vegetation. Nelson (1983) delineated forest canopy changes due to gypsy moth defoliation in Pennsylvania more accurately with vegetation index differencing than with other single band differencing or band rationing. Banner and Lynham (1981) on the other hand did not get good results when they used this algorithm in trying to delineate forest cutover owing to the sensitivity of NDVI to grass growth and the development of other vegetation in the clear-cuts. However, they found it useful in monitoring vegetation composition within the cutovers.

Serneels et al (2001) applied double univariate image differencing in a spatial-contextual approach to successfully separate anthropogenic changes from climate variability in a savanna environment in Kenya.

To improve the performance of this algorithm, several data pre-processing methods have been suggested. Hame (1986) suggested histogram matching and Yasuoka (1988) suggested band-to-band normalization before differencing TM data so as to yield bands with comparable means and standard deviations and to reduce scene-dependent effects. Coppin and Bauer (1994) suggested a standardization of the differencing algorithm to minimize the occurrence of identical change values depicting different change events. In the present study, the normalization of the NDVI images was undertaken by use of linear regression equation resulting from the mean NDVI values of the pseudo invariant features (PIFs) in the images.

4.2. Methodology.

4.2.1. Univariate NDVI image differencing.

The univariate NDVI image differencing analysis was performed using NDVI images of all the different dates. Various studies have adopted different approaches in NDVI image differencing analysis. Serneels et al (2001) for example, in their study of land cover changes in the Mara savanna ecosystem in Kenya. In their study, they used a combination of time contextual and spatial contextual approach to delineate areas of vegetation changes in the Mara savanna ecosystem. The technique computed and combined changes at pixel and landscape levels. First, they applied univariate image differencing to pairs of smoothed (101 x 101 pixel low-pass filter) vegetation index images to delineate large-scale changes. Second, the local scale patterns were detected via pixel-level image differencing between the two original (un-smoothed) full resolution images. Finally, the latter change image was subtracted from the former, resulting in a change image wherein all pixels that behaved differently over time at both scales had the highest change value.

In this study, only the time contextual approach was adopted (Figure 4.1). Here the image differencing technique was applied to pairs of multi-date images, subtracting NDVI values measured at successive dates. This band differencing method measures change along a continuum of change intensity. The difference depicts the degree to which the vegetation cover was modified. However, this method requires selection of a threshold to differentiate change from non-change (Fung and LeDrew, 1988). Two methods are often used for selection of thresholds (Singh, 1989): (1) Interactive procedure or manual trial-and-error procedure- analyst interactively adjusts threshold and evaluates the resulting image until satisfied, and (2) statistical measures- selection of a suitable standard deviation from a class mean. In this study, an interactively defined threshold was applied to make sure that only areas of high change intensities are retained in the final change map. The thresholds allowed classification of each difference image into three categories: increase in NDVI, no change, and decrease in NDVI-corresponding with increases in land cover, no change in land cover and decrease in land cover respectively.

To validate the detected change trajectories, the author visited the study area to gain ground-truth information about what was happening in the areas that appeared in the change trajectories.

Figure 4.1: Flow chart describing the time-contextual approach used to detect land cover changes in the KCA (Modified from Serneels et al. 2001).

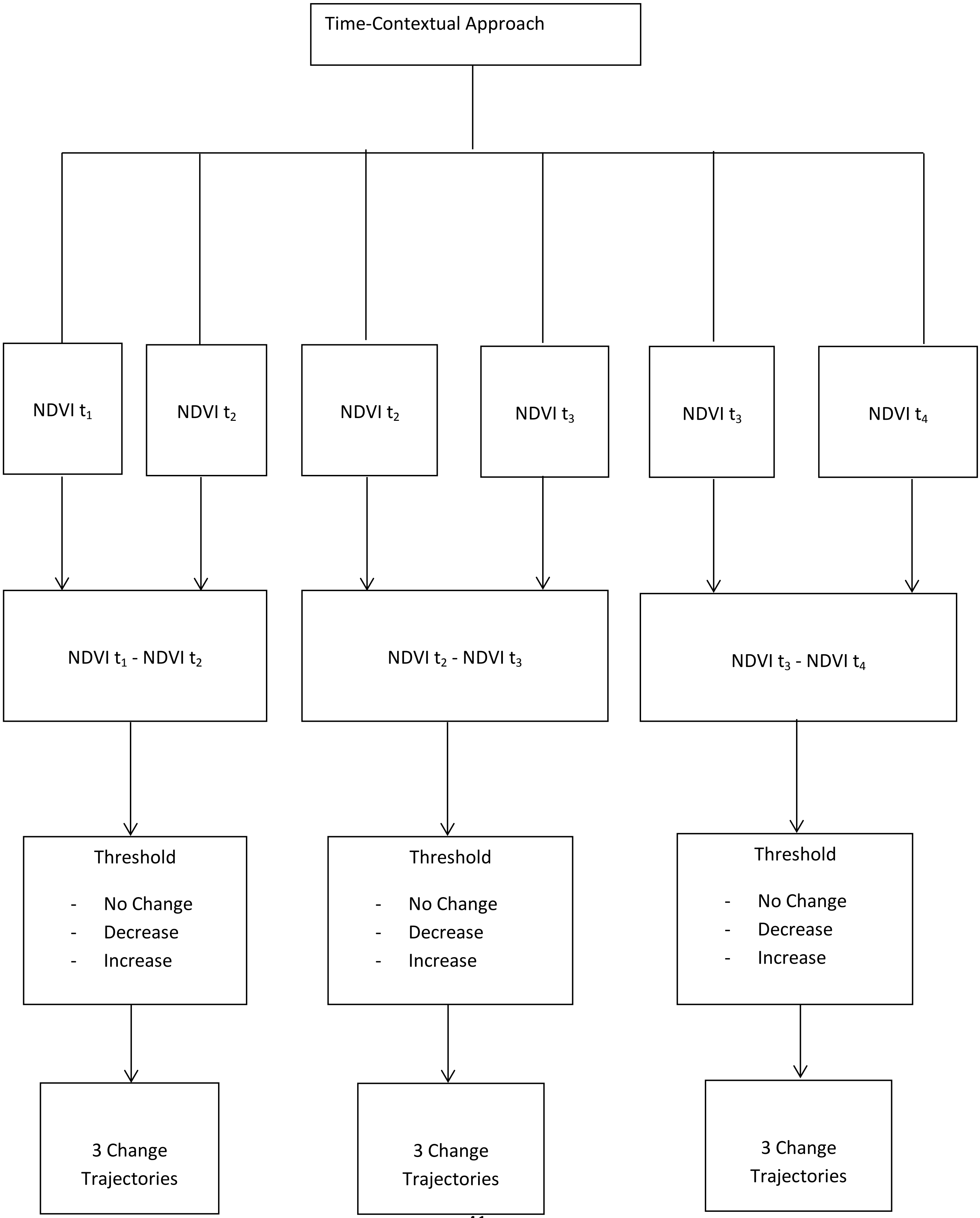

In the following sections, the results of the univariate image differencing analysis are presented. Note that in this chapter land cover changes are equated to changes in NDVI values (i.e. increase in NDVI values is equivalent to increase in land cover and vice versa).

4.3 Results

4.3.1 Land cover change trajectories in the KCA between 1986 and 1991

Figure 4.2 shows the land cover change map from the Landsat 1986 and 1991 TM data. After production of the change image, a threshold of 20% was applied to it so as to ensure that only areas of significant changes were highlighted in the final change map.

The area did not experience significant changes in vegetation greening. Some areas in the southeast appeared to have increased in NDVI values. Clouds are however suspected to play a part in the increases. Further interrogating is necessary to factor out the contributions of cloud cover, in order to generate a highly accurate assessment of vegetation cover in the area.

Fig. 4.2 NDVI Image Differencing for 1986 - 2001

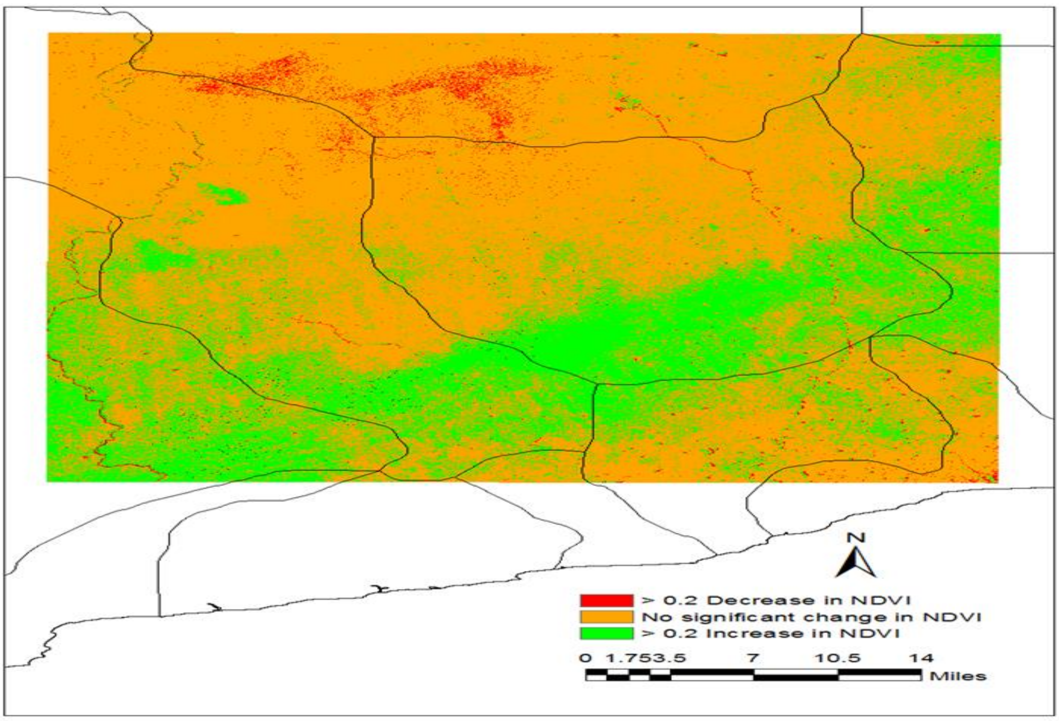

4.3.2 Land cover change trajectories in the KCA between 1991 and 2001.

Figure 4.3 below clearly shows an increase in greening (higher NDVI values) in the northwestern and middle portions of the KCA, outside the main protected forests. This largely could be associated to vegetation regrowth in highly cultivated agricultural lands around the protected forests.

It should be pointed out however that owing to time differences (fig. 2.1) on acquisition of respective images, caution must be exercised in drawing highly conclusive statements from the results. Further in-depth analysis is needed to remove remaining noise from remote sensing data through more robust pre-processing routines.

Fig. 4.3 NDVI Image Differencing for 1991 - 2001

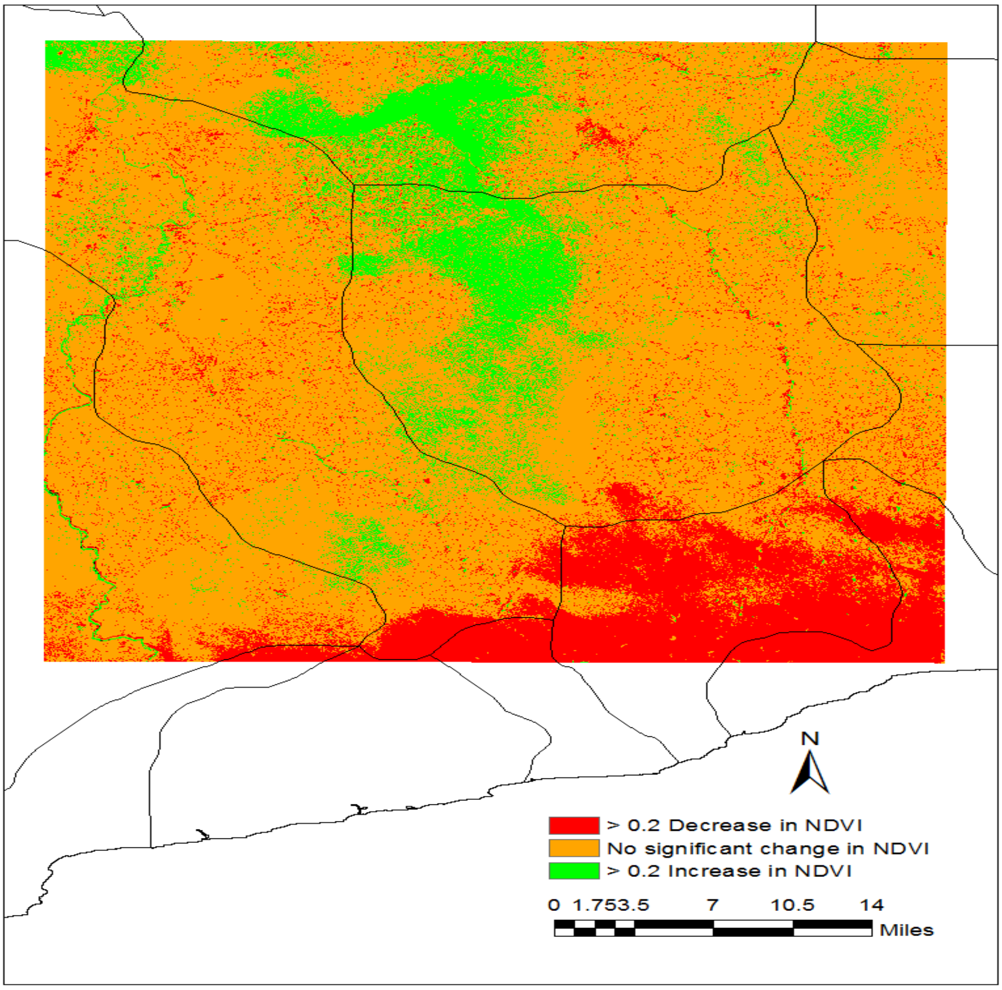

4.3.3 Land cover change trajectories in the KCA between 2001 and 2013.

The KCA in general and the Kakum-Attandanso forests experienced no noticeable vegetation change between 2001 and April 2003, as depicted in figure 4.4 below. However, various parcels especially in close proximity to the main protected forests saw increases in NDVI values. This may largely be due to increase agricultural activities in the area.

Fig. 4.4 NDVI Image Differencing for 2001 – 2013

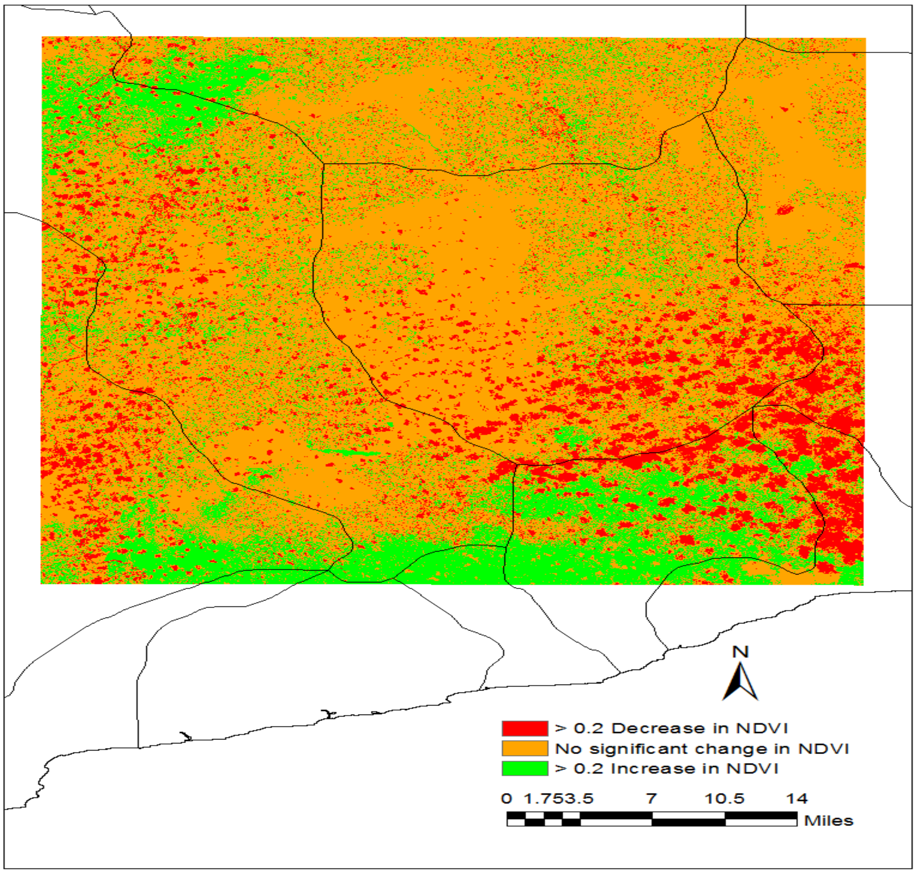

From the analyses of the results to determine the extent of observed change trajectories, it is evident that areas surrounding the main Kakum forest ecosystem especially, had undergone some form of land cover change over the period between 1986 and 1991. The land cover changes were either in terms of increase or decreases in NDVI-used as a proxy for measuring the trajectory of land cover change in this study.

In terms of spatial location of the observed land cover changes (Figure 4.4), some of the areas that experienced significant decrease in land cover include: The north-western part of the area. The southwestern areas however showed significant increases in land cover. But this might be impacted upon by clouds.

4.4. Discussion.

The univariate NDVI image differencing method was able to highlight areas that had experienced significant land cover changes in the study area over the study period and also the direction of these changes. From the 1986 and 1991 NDVI difference image, the results showed that the total area of the KCA had experienced some form of land cover change.

Based on the knowledge of the land use practices gained during fieldwork, a number of explanations can be put forward for the observed changes in land cover status that were observed in the difference images of the area. It is evident that most of the areas that experienced decrease in land cover between 1986 and 1991 are located in the southwestern part and this is an area that has experienced a tremendous immigration of agro-communities over time. It is therefore, logical to argue that as a result of this immigration, a number of areas were cleared of vegetation between these two dates to give room for cultivation agriculture. A field visit to this region by the author revealed that indeed most of this region is currently under cultivation agriculture.

Turning to the difference image between the 1991 TM and 2001 ETM+, it is evident that there were significant changes in land cover status of KCA with and area extent of 366km^2 experienced some form of land cover modification. Similar explanations to those put forward for the changes between 1986 and the 1991 also apply to the case of image differencing between 1991 and 2001. For example, in the south-western part of the area, some areas still showed remarkable decrease in land cover between 1991 and 2001. As was for the case with the 1986 and1991 difference image, the explanation here is that more vegetation is still being cleared to give room for cultivation agriculture. However, interestingly some of the cultivation zones were actually recorded as had undergone an increase in land cover between 1991 and 2001.The reason for the observation is linked to the type of cultivation agriculture being practiced in some of these areas. In some of the areas, farmers have been encouraged over the past to practice agro-forestry type of farming whereby trees are planted together with crops. This could provide the reason as to why these areas seem to have had an elevated NDVI instead of a reduction as would have been expected when forests are cleared and replaced by farms. Furthermore, in some of these areas, plantation forestry is being practiced and this would definitely lead to an increase in NDVI values in such farms.

4.5. Conclusion.

From the foregoing results and discussion, it is evident that the univariate NDVI image differencing algorithm was quite successful in discerning the land cover change trajectories that occurred in KCA during the entire study period. It is evident that the changes in land use and land acquisition arrangements I the study area have had a considerable impact on its land cover status. The notable land use practices that played a major role in these land cover dynamics include cultivation agriculture undertaken by the communities which immigrated into the area, increased cocoa agriculture and land acquisition arrangements.

In conclusion, it is worth noting that these results of NDVI image differencing show a very similar trend to those observed in the results of PCA in chapter three. It can therefore be stated that these two methods complement quite well and could offer a comprehensive means of studying land cover dynamics in forest ecosystems.

CHAPTER FIVE

EVALUATION OF THE TRENDS IN LAND COVER CHANGES IN THE MAJOR LAND COVER TYPES OF THE KCA.

5.1. Introduction.

In chapters three and four, the areas of possible land cover changes were identified and the trajectories for these changes were determined respectively. To be able to determine which land cover was affected by the observed changes and by how much, post-classification comparison of the land cover types between the study dates was deemed necessary. This required that the images be classified independently and then their land cover categories compared. However, it should be noted that production of a detailed classification map was not the main objective of this process, but rather a more general classification based on the dominant physiognomic characteristics of the vegetation types (tropical forest) of the KCA.

Post classification comparison involves independently produced spectral classification results from each end of the time interval of interest, followed by a pixel-by-pixel or segment-by segment comparison to detect changes in cover type. By adequately coding the classification results, a complex matrix of change is obtained, and change classes can be defined by the analyst. The principal advantage of post-classification comparison lies in the fact that the two dates are separately classified, thereby minimizing the problem of radiometric calibration between dates. The method can also be made insensitive to a variety of types of transient changes in selected terrain features that are of no interest by choosing the appropriate classification scheme. However, the accuracy of the post - classification comparison is totally dependent on the accuracy of the initial classifications. The final accuracy closely resembles that resulting from the multiplication of the accuracies of each individual classification and may be considered intrinsically low.

Nevertheless, several studies have used post-classification comparison method in change detection with some levels of success. For example, Hull et al (1991) classified Landsat images acquired at two different dates into five forest classes (clearings, regeneration, broadleaf, conifer, and mixed). Following the two classifications, they were able to construct a matrix of class changes and calculate the transition rates between the classes. Xu and Young (1990) on the other hand preceded their post-classification comparison by a manual segmentation of the images according to ground features and characteristics of the scene. They then classified all segments separately for each date via a supervised maximum likelihood pattern recognition routine. Through this procedure they were able to avoid some obvious errors in classification such as classifying moorlands as built-up in the case of their study.

In the present study, the basic classification approach was adopted and the results were later compared for each satellite image.

5.2. Methodology.

In the classification approach adopted, each image was classified using the unsupervised classification approach. A supervised classification was not done due to the lack of necessary ground data such as GCPs.

Finally, after the classification of each image, they were imported into the ArcMap Catalogue package to generate maps which were used to compare each image date to ascertain the amount of individual land use type change in the KCA over time.

5.3 Classification Results of the 1986, 1991, 2001 and 2013 Landsat Images

Figures 5.1 to 5.4 below present the classification results for all the images. Based on visual inspection of the original images and the available ancillary data, the final classification was categorized into five major physiognomic classes:(1) Forests (2) Agriculture (3) Bush/shrubland (4) Built-up/bare ground, and (5) Plantation.

Agricultural activities are hugely concentrated in the northern portion of the forest (see fig. 5.1) in the 1986 image. But these activities are evenly distributed and increased all around the protected forests of Kakum –Attandanso (see fig. 5.2 below), in the 1991 image in comparison with the 1986 image.

Fig. 5.1 Classification Map of the 1986 Landsat TM Image

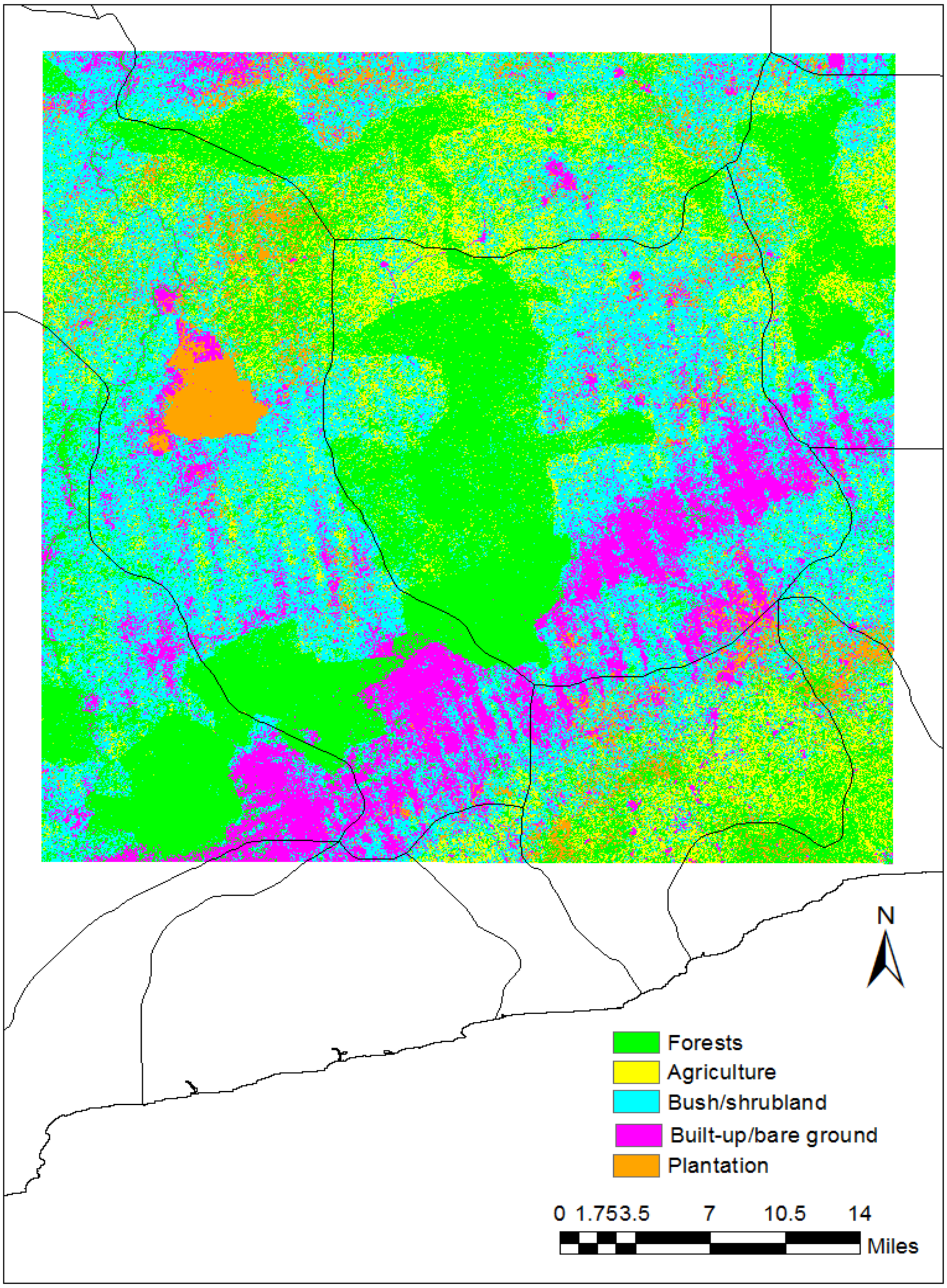

Fig. 5.2 Classification Map of the 1991 Landsat TM Image

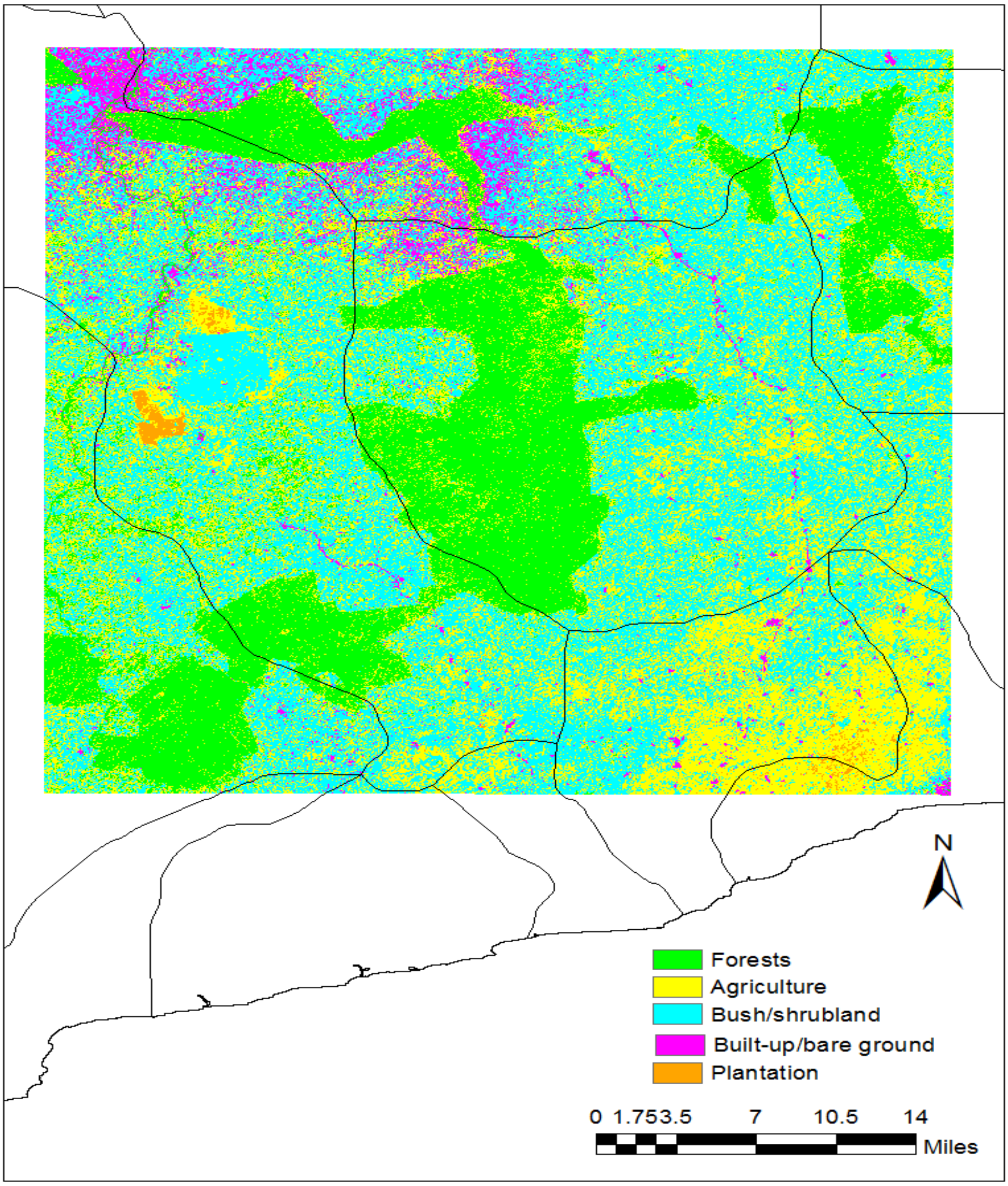

Fig. 5.3 Classification Map of the 2001 Landsat ETM Image

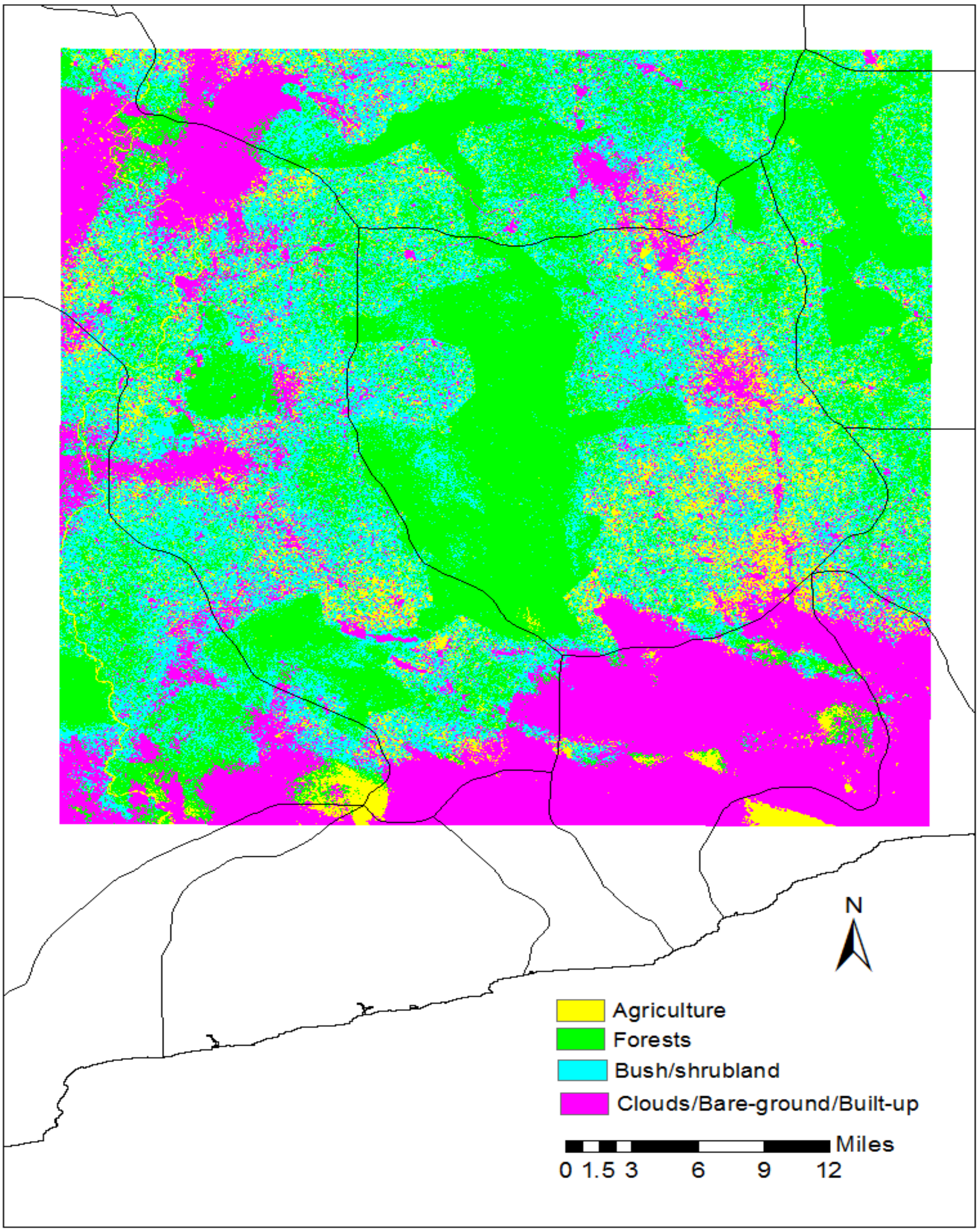

Fig. 5.4 Classification Map of the 2013 Landsat ETM Image

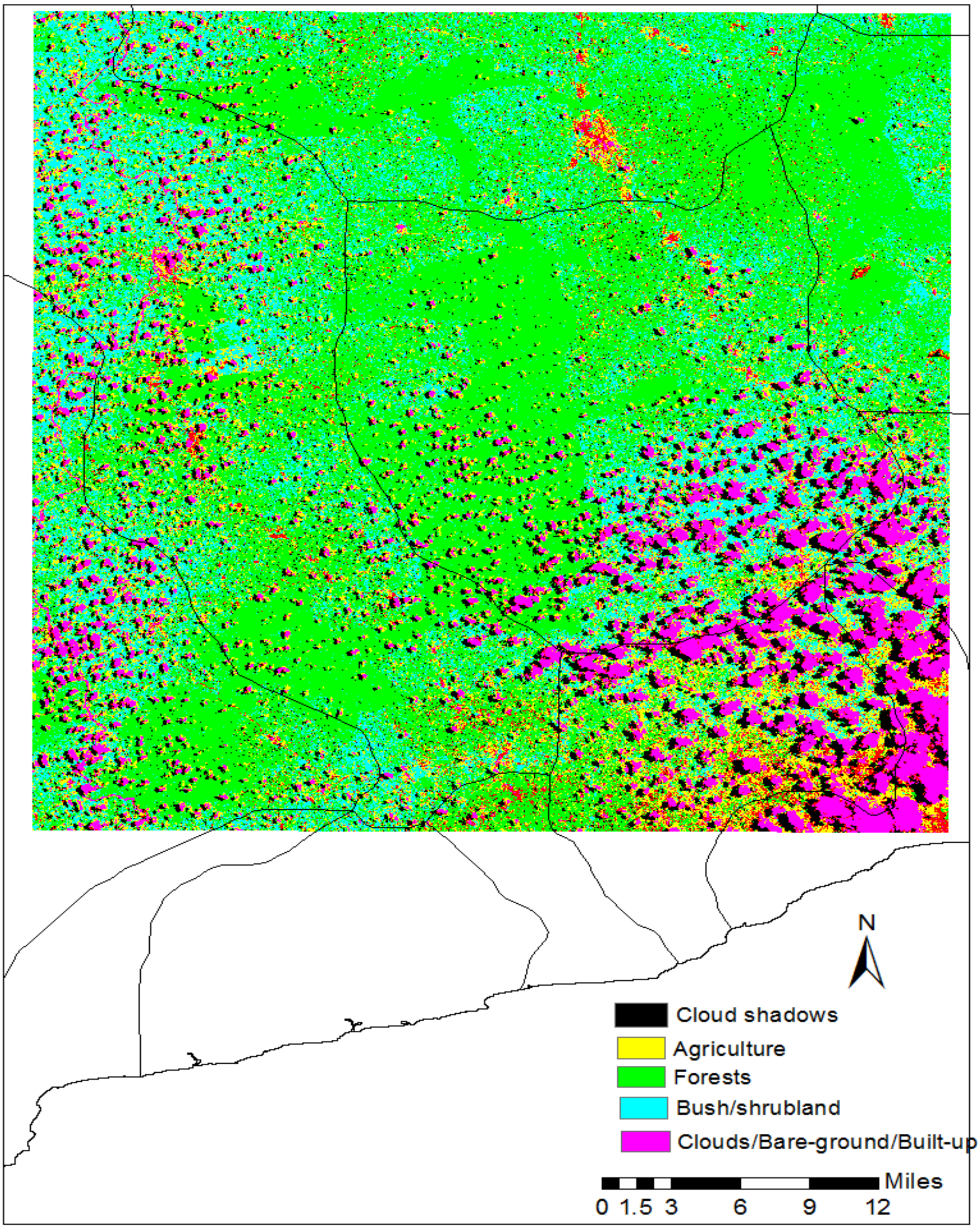

5.4 Discussion.

As the classification procedure was only intended at giving a general picture of the land cover changes in KCA over the study period, it is evident that the results were plausible. Looking at the maps of the various land cover types over the years (Figures 5.1, 5.2, 5.3 &5.4), it is clear that the forest and riverine vegetation category has been undergoing a gradual decline in cover from 1986 to 2013. This is understandably so since these regions have fertile soils and reliable rainfall suitable for cultivation agriculture and hence would be the first target for the immigrating agro-communities in the area. Indeed the classification maps have shown that the amount of forest and riverine vegetation category had declined from 1986 steadily to 2013.

The trend in the vegetation cover decline continued between 2001 and 2013, but at a much more slower rate. A reason for this slow decline could possibly be the type of agriculture that has been encouraged in the area. Agro-forestry and plantation forestry have been encouraged in the regions where cultivation agriculture is being practiced. This could have led to those areas that were initially classified as cultivated lands before the introduction of agro-forestry being classified as forests after the inception of the practice and hence reducing the detectable change from forests into cultivation agriculture.

In the category of cultivated land, bare ground and degraded zones, through both visual inspection and unsupervised classification signatures, 1986 image seemed to have had very minimal/undetectable cover under this category. However, in 2001 this increased evidently. This is due to the fact that this period experienced an enormous immigration of agro-communities into the area, particularly in the western and eastern portions. They then engaged in the clearance of the forested areas to give room to cultivate land. Between 2001 and 2013, there was a slight decline in the area categorized as cultivated, bare ground and degraded zone. This might have resulted from the reason mentioned earlier, that is, the introduction of agro-forestry and plantation forestry in some of the areas previously classified as cultivated lands in the 2001 image being classified as forests in the 2013 image.

Image artefacts, especially cloud cover have had influence on built up and bare-ground area analysis in the 1986 image (Fig. 5.1). Much more robust image processing regime is required to remove or reduce the impacts of such image artefacts in order to make the results and analysis much rigorous and representative.

Similar challenges from cloud artefacts (which could not be removed completely by the Atmospheric correction algorithm adopted), present a huge source of bias into the analysis of bare-ground and built up areas. The south-eastern corner of both the 2001 and 2013 images by visual inspection reports huge changes in that land use type. Though visits to the area during fieldwork showed some bare-ground and built up expansion, especially in some main townships, what is reported does not depict the true picture on the ground, and could only be attributable to cloud bias.

5.5. Conclusion.

The results of the classification of the satellite images were quite plausible. They indicated that the changes in land use systems in KCA have had a dramatic influence on the land cover dynamics of the entire study area. Cultivation agriculture is on the rise as more and more of the area is being sub-divided into individual leases and share-cropping arrangements. The land cover type that seems to bear the brunt of the onslaught of cultivation agriculture is the forests and riverine vegetation. The reason for this is that these areas have both fertile soils and reliable rainfall as opposed to other parts of the area.

It can therefore be concluded that considering that the classification was performed without adequate ancillary data (due to the retrospective nature of the images and accessibility) and with the problem of mixed pixels, they were able to give a fair account of how the changes in land use practices and land tenure systems have impacted on the trends of the major land cover categories of the KCA.

CHAPTER SIX

GENERAL CONCLUSIONS

6.1. Overview

The study sets out to examine the possible land cover dynamics that had taken place in the KCA as a result of changes in land use systems using an integration of remote sensing and GIS methods. Within this broad aim, the specific objectives were:

- To identify areas of this ecosystem that had undergone significant land cover changes,
- To analyze and map the land cover change trajectories in this ecosystem,
- To classify available satellite images and use the classification maps to identify trends of land cover changes in each land cover type and,
- To provide possible reasons for the observed land cover changes where appropriate.

Three methodologies were adopted to achieve these objectives: (1) principal components analysis (PCA), (2) univariate NDVI image differencing and (3) classification analyses. Principal components analysis was used to detect the areas that had experienced possible land cover changes over the study period. After highlighting these areas, it was deemed necessary to determine whether they were increases or decreases in land cover. The univariate NDVI image differencing algorithm was used to determine these change trajectories. Finally, classification of all the satellite images was undertaken and the resultant image classification maps compared to gain knowledge of the trends of the observed land cover changes in each land cover type.

6.2. Findings

It was evident that the land cover of KCA had undergone considerable changes over the study period. Principal components analysis was able to identify areas of possible land cover changes in the area. The algebraic patterns of the loadings in the eigenvectors of the various principal components (PCs) were examined to identify those PCs that seemed to depict areas of change (i.e. PCs which had negative loadings on the channels of one date and consequent positive loadings on the channels of the second date). In this study, PC2 and PC4 on both the two merged data sets seemed to highlight areas of possible land cover changes. A visual analysis of these PCs showed that there were regions which had significant departures from the grey scale (i.e. either elevated brightness or high levels of dark tones), a phenomenon that has been shown to indicate areas of possible change in land cover change detection studies using PCA (Byrne et al, 1980; Fung and LeDrew 1987).

The location of these areas was determined and visited during fieldwork to find out what was going on in terms of the current land use practices. It was apparent that the south-western region of the area (an area presently under cultivation agriculture) and the north eastern region appeared as areas that had undergone some form of land cover changes from the PCA results. In order to determine what these changes were, the NDVI image-differencing algorithm was then implemented on the NDVI images of each of the satellite images.

The results from the PCA in chapter three clearly showed that there have been vegetation cover changes between the years. The first and second PCs together representing the accumulated greenness. As utilized by Hirosawa, Y. et al (1996) in the application of PCA to land cover characterization using multitemporal AVHRR Data, all the three PCA matrices in this study (Tables 3.1, 3.3 & 3.5) presented values of the first PC eigenvectors to be positive, higher and consistent over the entire analysis. The second PCs on the other hand showed a somewhat cyclical pattern or seasonal variation. It can therefore be explained that PC1 eigenvalues in all the individual periods (Tables 3.2 (73.5%), 3.4 (71.56%) and 3.6 (83.51%)), serve to quantify the density and photosynthetic activity of vegetation. The values of PC2 also quantify the seasonal patterns of vegetation change.

The univariate NDVI image differencing results were able to highlight the specific land cover change trajectories that occurred in the KCA over the study period. It was also deduced that the areas that had undergone either increases or decreases in land cover had been influenced in one way or the other by the land use practices in those particular regions. For example, the southwestern part immigration of agro-communities into these regions who have been clearing these zones to give way to cultivation agriculture (mainly cocoa agriculture) and expansion of settlements.

From the results of classification of the images, it was deduced that over three-quarters (3/4) of the area is under the land cover category-tropical forest. In terms of land cover changes; the forested regions seem to have undergone a significant decline over the study period, mainly around the protected Kakum-Attandanso forest. This is due to the fact that these areas have fertile soils and reliable rainfall and would therefore be the first target areas for immigrating agricultural-based communities.

Overall it suffices to say that the effect of noise, especially that of clouds, which could not be removed completely by the DOS atmospheric correction algorithm applied, might have introduced some negative biases in the results. Nonetheless, the study has proved the significance of remote sensing and GIS capabilities in land cover change analysis. More robust atmospheric correction algorithms such as FLAASH, need to be adopted to improve upon the accuracy level of the results.

In conclusion, judging by these results, it can be said that the integration of remote sensing and GIS proved viable in detecting the land cover dynamics that have occurred in the KCA as a result of changes in land use and land tenure systems. GIS and remote sensing therefore offers a viable alternative to studying landscape dynamics in vast ecosystems such as the tropical forest where traditional land cover studies would be inadequate and uneconomical.

6.3. Further research.

Areas of further research and consideration should aim at looking at how to improve image processing quality as the KCA is bedevilled with an extensive cloud cover over a larger part of the year. Thus much more robust and in-depth image processing algorithms (Example, FLAASH and QUAC in the ENVI software) to isolate attributes such as clouds, which might impact hugely on results (see Mayaux, P. et al, (2013))

Another processing issue is that of mixed land cover composition, making land use analysis and evaluation complicated. Applications such as the one adopted by Foody, G.M. et al (1997) in mapping tropical forests in the Mato Grosso area in Brazil, could be employed to increase the robustness of land use and land cover analyses in the KCA and other similar regions.

REFERENCES

Abd El-Kawy, O.R. et al (2011) Land use land cover change detection in Western Nile delta of Egypt using remote sensing data. *Applied Geography, 31:483-494*.

Allotey J. (2007), Status of biodiversity and impact assessment in Ghana. *Biodiversity and Impact Assessment. Doc/ED'sDoc/26/04/2007.*

Anim-Kwapong, G.J. and Frimpong, E.B. (2005), Vulnerability of Agriculture to Climate Change on Cocoa Production: Vulnerability and Adaptation Assessment under the Netherlands Climate Change Studies Assistance Programme Phase (NCCSAP2).

Appiah, M., Blay, D., Dannyag, H., Dwomoh, F.K., Pappien, A. and Luukkanen, O. (2009), Dependence on forest resources and tropical deforestation in Ghana. *Environment, Development and Sustainability, Volume 11, Issue 3, pp. 471-487*.

Asenso-Okyere, K. (2001), Transforming Agricultural production and productivity for sustained rapid growth and development. In: Ghana in the 21st Century. ISSER millennium seminar series, No. 4. Institute of Statistical, Social and Economic Research (ISSER), University of Ghana. 34pp.

Asner G.P. (2009), Tropical forest carbon assessment: integrating satellite and airborne mapping approaches. *Environ. Res. Lett. 4 034009 1-11*.

Asner G.P. (1998) Biophysical and Biochemical Sources of Variability in Canopy Reflectance. *Remote Sensing of Environment, 64: 234-253*.

Auzins, A. (2004), Institutional Arrangements: A Gate towards Sustainable Land Use, Nordic *Journal of Surveying and Real Estate Research, Vol. 1, pp57-71*.

Bernstein, L.S., et al (2006) Improved Reflectance Retrieval from Hyper- and Multispectral Imagery without Prior Scene or Sensor information. *SPIE Proceedings, Remote Sensing of Clouds and the Atmosphere XI. Vol. 6362.*

Bernstein, L.S., et al (2005) Validation of the Quick Atmospheric Correction (QUAC) algorithm for VNIR-SWIR multi- and hyperspectral imagery. *SPIE Proceedings, Algorithms and Technologies or Multispectral, Hyperspectral, and Ultraspectral Imagery XI. Vol. 5806, pp 668-678.*

Brown S. et al (2005), Creating a virtual tropical forest from three-dimensional aerial imagery to estimate carbon stocks. *Ecol. Appl. 15 1083-95.*

Campbell, J.B (2002) Introduction to Remote sensing (3rd Ed). Taylor and Francis Ltd. London.

Campbell, J.B. and Liu, X. (1995). Chromaticity Analysis in Support of Multi-spectral remote sensing: In proceedings, ACSM/ASPRS Annual Convention and Exposition. American Society for Photogrammetry and remote sensing. Bethseda. M.D.

Clark M.L. et al (2011), Estimation of tropical rainforest aboveground biomass with small-foot print lidar and hyperspectral sensors. *Remote Sensing of Environment 115 2931-2942.*

Chape S, et al (2005) Measuring the extent and effectiveness of protected areas as an indicator for meeting global biodiversity targets. *Phil. Trans. R. Soc. B, 360, 443–455.*

Chavez, P.S. Jr. (1996). Image-based atmospheric corrections-revised and improved. *Photogrammetry engineering and remote sensing. 62, No.9 pp 1025-1036.*

Coppin, R.D, Jonckheere, J. Nackaetts, K., Muys, B and Lambin, E. (2004). Digital change detection methods in ecosystem monitoring: a review. *International journal of remote sensing 25, 1565-1596*.

Coppin, P.R., and Bauer, M.E. (1994). Processing of multi-temporal Landsat TM imagery to optimise extraction of forest cover change features. *IEEE Transactions on geoscience and remote sensing 32, 918-927*.

Cote, I.M. & Darling, E.S. (2010) Rethinking Ecosystem Resilience in the Face of Climate Change. *PLoS Biology, Vol.8, 7, 1-5*.

Crippen, R.W. (1989). A simple spatial filtering routine for the cosmetic removal of scan line noise from Landsat TM p-tape imagery. *Photogrammetry Engineering and Remote sensing 50 No. 3 pp 343-352*.

Curran, P. (1980) Multispectral remote sensing of vegetation amount. *Progress in Physical Geography, 4: 315*.

Estes, J.E., Stow, D., and Jensen, J.R. (1982). Monitoring land use and land cover changes: Remote sensing for resource management: In C. Johannsen and J. Sanders, editors.) Soil conservation society of America, Iowa. Pp. 100-110.

Falkowski et al. (2000), The Global Carbon Cycle: A test of our understanding of our knowledge of the earth as a system.

FAO 2010. Global Forest Resources Assessment. Main report. FAO Forestry Paper 163. Food and Agriculture Organization of the United Nations, Rome, Italy.

FAO (2005), Global Forestry Resource Assessment. FAO Forestry Paper 147, Rome.

Fischlin, A., G.F. Midgley, J.T. Price, R. Leemans, B. Gopal, C. Turley, M.D.A. Rounsevell, O.P. Dube, J. Tarazona, A.A. Velichko, 2007: Ecosystems, their properties, goods, and services. Climate Change 2007: Impacts, Adaptation and Vulnerability. Contribution of Working Group II to the Fourth Assessment Report of the Intergovernmental Panel on Climate Change, M.L. Parry, O.F. Canziani, J.P. Palutikof, P.J. van der Linden and C.E. Hanson, Eds., Cambridge University Press, Cambridge, 211-272.

Folke et al. (2005), Adaptive Governance of Social-Ecological Systems. *Annual Review Environ. Research, 30: 441- 473.*

Foody, G.M. et al (1997) Mapping Tropical Forest fractional cover from coarse spatial resolution remote sensing imagery. *Plant Ecology, 131, 143-154.*

Fung, T. and LeDrew, E., (1988). The determination of optional threshold levels for change detection using various accuracy indices. *Photogrammetric engineering and remote sensing, 54. 1449-1454.*

Fung, T., and LeDrew, E., (1987). Application of principal components analysis to change detection. *Photogrammetry engineering and remote sensing, 1649-1658.*

Geldmann, J. et al. (2013) Effectiveness of terrestrial protected areas in reducing habitat loss nd population declines. *Biological Conservation, 161: 230-238.*

Gibbs H.K. et al (2007), Monitoring and estimating tropical forest carbon stock: making REDD a reality. *Environ. Res. Lett. 2 045023.*

Glaser, M. (2006), The Social Dimensions in Ecosystems Management: Strengths and weaknesses of Human-Nature Mind-Maps. *Human Ecology Review, Vol. 13, No.2.*

GLCF: http://www.landcover.org/index.shtml (Accessed on the 10/05/2013).

Glovis: http://glovis.usgs.gov (Accessed on the 01/05/2013).

Hall, F.G., Botkin, D., Strebel, D., Woods, K.D., and Goetz, S.S., (1991). Large-scale patterns of forest succession as determined by remote sensing. *Ecology 72, 628-640*.

Hame, T.H. (1986). Satellite image aided change detection. In remote sensing aided forest inventory, Research notes No. 19. Dept. of Forest Mensuration and Management, University of Helsinki, Helsinki, Finland. Pp 47-60.

Henebry, G.M (1997). Advantages of principal components analysis for land cover segmentation from SAR image series. Proceedings of the 3rd International ERS Symposium.

Hirosawa, Y., et al (1996) Application of Standardized Principal Component Analysis to Land-Cover Characterization Using Multitemporal AVHRR Data. *Remote Sen. Environ. 58: 267-281*.

Holmes, A. McR., et al (1987). The development of a system for monitoring trend in range condition in the arid shrublands of Western Australia. *Australian Rangeland Journal 9: 14-20*.

Ingebitsen, S.E., and Lyon, R.J., (1985). Principal components analysis of multi-temporal image pairs. *International journal of remote sensing, 6 No 5 pp 687-696*.

IUCN/PACO (2010) Parks and reserves of Ghana: Management effectiveness assessment of protected areas, Ouagadougou, BF: IUCN/PACO.

Jachmann, H. (2008) Illegal wildlife use and protected area management in Ghana. *Biological Conservation, 141, 1906-1918*.

Kpelle, D.G. (1993), Evaluation of Past Management and Resource Use of the Kakum and Assin-Attandanso Forest Reserves. Unpublished Report, Department of Wildlife, Accra.

Kramer, E.A., Restrepo, C. and Moritz, C. (1997), Tropical Forest Fragmentation: Synthesis of a Diverse and Dynamic Discipline in: Laurance, W.F. and Bierregard, R.O. Tropical Forest Remnants Ecology, Management, and Conservation of Fragmented Communities, Chicago University Press, Chicago 616 pp.

Kwarteng, A.Y., and Chavez, P.S. (1998). Change detection study of Kuwait city and environs using multi-temporal Landsat thematic data. *International journal of remote sensing 19, 1651-1662*.

Lambin, E.F., and Strahler, A.H., (1994). Change-vector analysis: A tool to detect and categorize land cover change processes using high temporal resolution satellite data. *Remote sensing of environment, 15, 2099-2119*.

Landsat 7. (2011). Landsat 7. Science data Users Handbook. Chapter 11. Data products. Landsat Technical Notes. 1, 3-7.

Lansing, J.S. (2003), Complex adaptive system. *Annual Rev. Anthropology. 32: 183-204*.

Liang, S., Fang, H., and Chen, M., (2001). Atmospheric correction of Landsat ETM+ land surface imagery-part 1: Methods. *IEEE Transactions of geoscience and remote sensing, 39, 2490-2498*.

Lillesand, T.M., and Kiefer, R.W. (2000) Remote sensing and image interpretation 4th Edition. John Wiley and Sons Inc. New York.

Liverman, D. et al (1998) People and Pixels: Linking Remote Sensing and Social Science. National Academy Press, Washington, D.C.

Lu D., Mausel P., Brondizos E., and Moran E., (2004). Change detection techniques. *International journal of remote sensing. Vol. 25, No. 12, 2365-2407*.

Ludwig, D., Mangel, M. & Haddad, B. (2001), Ecology, Conservation and Public policy, *Annual Rev. Ecol. System, 32: 481-517.*

Luneta, R., and Elvidge, C. (1999). Remote sensing change detection: environmental monitoring methods and applications. Taylor and Francis, London.

Lyon, J., Yuan, D., Lunetta, R., and Elvidge, C., (1998). A change detection experiment using vegetation indices. *Photogrammetric engineering and remote sensing. 64, 143-150.*

Malhi, Y. (2010), The Carbon Balance of Tropical Forest Regions, 1990- 2005. Current opinion in Environmental Sustainability 2010, 2: 237-244.

Malhi Y. et al (2010), Introduction: Elevation gradients in the tropics: laboratories for ecosystem ecology and global change research. *Global Change Biology 16, 3171-3175.*

Malila W.A. (1980). Change vector analysis: an approach to detecting forest changes with Landsat. Proceedings of the 16th International symposium on Machine proceeding of remotely sensed data, Purdue University, West Lafayette, pp326-335.

Markham, B.L., and Chander, G., (2003). Revised Landsat 5 TM radiometric calibration procedures and post-classification dynamics ranges. EOSAT Landsat technical notes.

Markham, B.L. and Barker, J.L., (1986). Landsat MSS and TM post-calibration dynamic ranges, exo-atmospheric reflectances and at-satellite temperatures. EOSAT.

Mas, J. (1999). Monitoring land cover change: A comparison of change detection techniques. *International journal of remote sensing Vol. 20 No. 139-152.*

Mather, P.M. (1999). Computer processing of remotely sensed images, 2nd Edition. John Wiley and Sons. Chichester.

Mayaux, P. et al (2013) State and evolution of the African rainforests between 1990 and 2010. *Phil. Trans. R. Soc. B. 368: 20120300.*

Milne, A.K. (1988) Change detection analysis using Landsat Imaging: A review of methodology. Proceedings of the IGARSS 88 Symposium. Edinburgh, Scotland, ESASP-284.

Muchoney, D.M and Haack, B.N., (1994). Change detection for monitoring forest defoliation. *Photogrammetric engineering and remote sensing. Vol. 60 No, 10 pp 1243-1251.*

Nabuurs, G.J. et al (2007), Forestry. In Climate Change 2007: Mitigation. Contribution of WG III to the 4th Assessment Report of IPCC [B. Metz, O.R. Davidson, P.R. Bosch, R. Dave, L.A. Meyer (eds)], Cambridge University Press, Cambridge and New York, NY, USA

Nelson, R.F., (1983). Detecting forest canopy change due to insect activity using Landsat MSS. *Photogrammetric engineering and remote sensing 49, 1303-1314.*

Newton A. C. (2011) Social-ecological resilience and biodiversity conservation in a 900-year-old protected area. *Ecology and Society 16 (4): 13.*

Parrott, L. & Meyer, W. S (2012) Future Landscapes: managing within complexity. *Frontiers in Ecology and the Environment, 10, 382–389.*

Pickup, G., Chewing, V.H., and Nelson, D.J., (1993). Estimating change in vegetation cover over time in arid rangelands using Landsat MSS data. *Remote sensing and Environmet.15, 597-617.*

Richards, J.A., (1999) Remote Sensing Digital Image Analysis, Springer-Verlag, Berlin, p. 240.

Richards, J.A. (1984). Thematic mapping from multi-temporal image data using the principal components transform. *Remote sensing of environment, 16 pp 35-46*.

Roderick, M., et al (1996). Calibrating long term AVHRR-derived NDVI imagery. *Remote Sensing of Environment, 58: 1-12*.

Rouse, J.W. et al (1973). Monitoring vegetation systems in the Great Plains with ERTS, *Third ERTS symposium, NASA SP-351 1, 309-317*.

Rudel, T. (1999), Critical Regions, Ecosystem Management and Human Ecosystem Research.

Sabins, F.F. (1997). Remote sensing: principles and interpretation. 3rd Edition. W.H. Freeman and Company. New York.

Sarka, S. & Illoldi-Rangel, R. (2010), Systematic Conservation Planning: an Updated Protocol, *Natureza & Conservacao, 8 (1): 19-26*.

Serneels, S., Said, M.Y., and Lambin, E.F., (2001). Land cover changes around major East Africa wildlife reserve: the Mara Ecosystem (Kenya). *International journal of remote sensing 22, 3397-3420*.

Serra, P, Pons, X and Sauri, D., (2003) Post-classification change detection with data from different sensor: some accuracy considerations. *International journal of remote sensing*. *Vol. 24, No. 16. 1311-3340*.

Siljerstrom, R.P., and Lopez M.A. (1995). Monitoring burnt areas by principal components analysis of multi-temporal TM data. *International journal of remote sensing 16 pp 1577-1587*.

Singh, A (1989). Digital Change detection techniques using remotely sensed data. *International journal of remote sensing, Vol. 10. 989-1003*.

Skole, D. and Tucker, C. (1993), Tropical deforestation and habitat fragmentation in the Amazon: Satellite data from 1978 to 1988. *Science, 260: 1905-10*.

Srinivisan, R., Cannon M., and White J., (1988). Landsat de-striping using power spectral filtering. *Journal of Optical Engineering 27, No. 11 pp 939-943*.

Tou, J.T. and Gonzalez, R.C., (1974) Pattern Recognition Principles. *Addison-Wesley Publishing Company, Reading, Massachusetts*.

Thouless, C.R., and Sakwa, J., (1995). Shocking elephants: fencing and crop raiders in Laikipia district, Kenya. *Biological conservation, 72, 35-41*.

Tucker, C.J. (1986). Maximum normalized difference vegetation index for sub-Saharan Africa for 1983-1985. *International journal of remote sensing, 7, 1383-1384*.

Tucker, C.J. (1979). Red and photographic infrared linear combinations for monitoring vegetation. *Remote sensing of environment, 8, 127-150*.

UNEP (2006), Country Report: www.unep.org/pressrelease/Ghana_Africa (Accessed: 01/06/2013).

Verbury, P.H. et al (2009) From landcover change to land dynamics: A major challenge to improve land characterization. *Journal of Environmental Management, 90, 1327-1335*.

Wang, F. (1993). A knowledge based vision system for detecting land cover changes at urban fringes. *IEE Transactions on Geosciences and remote sensing 31: 136-145*.

Xu, H., and Young, J., (1990). Monitoring changes in land use through integration of remote sensing and GIS. *Proceedings of the IGARSS' 90 Symposium. University of Maryland, College Park, M.D. USA (Picataway, NJ: IEEE) pp 957-960*.

Yasuoka, Y., (1988). Detection of land cover changes from remotely sensed image using spectral signature similarity. *Proceedings of the 9th Asian Conference on Remote Sensing*. *November 1988, ppG31-G36*.